



## RESEARCH PAPER

# A novel cross-species inhibitor to study the function of CatSper Ca<sup>2+</sup> channels in sperm

**Correspondence** Timo Strünker, University Hospital Münster, Centre of Reproductive Medicine and Andrology, Münster, Germany.  
E-mail: timo.struenker@ukmuenster.de

**Received** 29 May 2017; **Revised** 14 April 2018; **Accepted** 20 April 2018

Andreas Rennhack<sup>1,\*</sup>, Christian Schiffer<sup>2</sup>, Christoph Brenker<sup>2</sup>, Dmitry Fridman<sup>1</sup>, Elis T Nitao<sup>3</sup>, Yi-Min Cheng<sup>4</sup>, Lara Tamburrino<sup>5</sup>, Melanie Balbach<sup>1</sup>, Gabriel Stölting<sup>6</sup> , Thomas K Berger<sup>1</sup>, Michelina Kierzek<sup>2</sup>, Luis Alvarez<sup>1</sup>, Dagmar Wachten<sup>8,7</sup>, Xu-Hui Zeng<sup>4</sup>, Elisabetta Baldi<sup>5</sup>, Stephen J Publicover<sup>3</sup>, U Benjamin Kaupp<sup>1</sup> and Timo Strünker<sup>2</sup> 

<sup>1</sup>Department of Molecular Sensory Systems, Center of Advanced European Studies and Research (CAESAR), Bonn, Germany, <sup>2</sup>University Hospital Münster, Centre of Reproductive Medicine and Andrology, Münster, Germany, <sup>3</sup>School of Biosciences, University of Birmingham, Birmingham, UK, <sup>4</sup>Institute of Life Science and School of Life Science, Nanchang University, Nanchang, Jiangxi China, <sup>5</sup>Department of Experimental and Clinical Medicine, Center of Excellence DENOTHE, University of Florence, Florence, Italy, <sup>6</sup>Institute of Complex Systems – Zelluläre Biophysik 4, Forschungszentrum Jülich, Jülich, Germany, <sup>7</sup>Max-Planck Research Group of Molecular Physiology, Center of Advanced European Studies and Research, Bonn, Germany, and <sup>8</sup>Institute of Innate Immunity, University Hospital, University of Bonn, Bonn, Germany

\*Present address: Concept Life Science, Sandwich, UK.

### BACKGROUND AND PURPOSE

Sperm from many species share the sperm-specific Ca<sup>2+</sup> channel CatSper that controls the intracellular Ca<sup>2+</sup> concentration and, thereby, the swimming behaviour. A growing body of evidence suggests that the mechanisms controlling the activity of CatSper and its role during fertilization differ among species. A lack of suitable pharmacological tools has hampered the elucidation of the function of CatSper. Known inhibitors of CatSper exhibit considerable side effects and also inhibit Slo3, the principal K<sup>+</sup> channel of mammalian sperm. The compound RU1968 was reported to suppress Ca<sup>2+</sup> signaling in human sperm by an unknown mechanism. Here, we examined the action of RU1968 on CatSper in sperm from humans, mice, and sea urchins.

### EXPERIMENTAL APPROACH

We resynthesized RU1968 and studied its action on sperm from humans, mice, and the sea urchin *Arbacia punctulata* by Ca<sup>2+</sup> fluorimetry, single-cell Ca<sup>2+</sup> imaging, electrophysiology, opto-chemistry, and motility analysis.

### KEY RESULTS

RU1968 inhibited CatSper in sperm from invertebrates and mammals. The compound lacked toxic side effects in human sperm, did not affect mouse Slo3, and inhibited human Slo3 with about 15-fold lower potency than CatSper. Moreover, in human sperm, RU1968 mimicked CatSper dysfunction and suppressed motility responses evoked by progesterone, an oviductal steroid known to activate CatSper. Finally, RU1968 abolished CatSper-mediated chemotactic navigation in sea urchin sperm.

### CONCLUSION AND IMPLICATIONS

We propose RU1968 as a novel tool to elucidate the function of CatSper channels in sperm across species.

### Abbreviations

2-AG, 2-arachidonoylglycerol; ABHD2,  $\alpha/\beta$  hydrolase domain-containing protein 2; ASW, artificial sea water; [Ca<sup>2+</sup>]<sub>i</sub>, intracellular Ca<sup>2+</sup> concentration; CASA, computer-assisted sperm analysis; HSA, human serum albumin; HTF, human tubal fluid; MES, 2-(N-Morpholino)ethanesulfonic acid; pH<sub>i</sub>, intracellular pH; sEBSS, supplemented Earle's balanced salt

solution; TAPS, N-[Tris(hydroxymethyl)methyl]-3-aminopropanesulfonic acid; TYH, Toyoda, Yokoyama and Hosi's; VAP, velocity average path;  $V_m$ , membrane potential

## Introduction

The intracellular  $Ca^{2+}$  concentration ( $[Ca^{2+}]_i$ ) modulates the beat of the sperm flagellum and, thereby, the swimming behaviour (Publicover *et al.*, 2008; Alvarez *et al.*, 2014). In many but not all species,  $[Ca^{2+}]_i$  is controlled by the sperm-specific  $Ca^{2+}$  channel **CatSper** (cation channel of sperm) (Quill *et al.*, 2001; Ren *et al.*, 2001; Kirichok *et al.*, 2006; Lishko *et al.*, 2010; Loux *et al.*, 2013; Seifert *et al.*, 2015). CatSper appeared early in evolution, before the branching of eukaryotes into unikonts and bikonts (Cai and Clapham, 2008; Cai *et al.*, 2014; Chung *et al.*, 2017). So far, most of our knowledge about CatSper originates from physiological studies of native channels in mammalian and sea urchin sperm. In general, CatSper is activated by depolarization of the membrane potential ( $V_m$ ) and by alkalization of the intracellular pH ( $pH_i$ ) (Kirichok *et al.*, 2006; Lishko *et al.*, 2010; Lishko *et al.*, 2011; Strünker *et al.*, 2011; Seifert *et al.*, 2015). In sea urchin sperm, the egg's chemoattractant evokes rapid changes in  $V_m$  and  $pH_i$ , stimulating  $Ca^{2+}$  influx via CatSper (Seifert *et al.*, 2015; Espinal-Enríquez *et al.*, 2017), which controls chemotactic steering. Targeted ablation of genes encoding CatSper channel subunits provided insight into the function of CatSper in mouse sperm (Quill *et al.*, 2001; Ren *et al.*, 2001; Carlson *et al.*, 2003; Carlson *et al.*, 2005; Liu *et al.*, 2007; Qi *et al.*, 2007; Wang *et al.*, 2009; Chung *et al.*, 2011; Zeng *et al.*, 2013; Chung *et al.*, 2017). For instance, sperm from CatSper<sup>-/-</sup> mice suffer from impaired motility (Ren *et al.*, 2001; Qi *et al.*, 2007; Miki and Clapham, 2013), fail to traverse the oviduct (Ho *et al.*, 2009; Miki and Clapham, 2013; Chung *et al.*, 2014), and are unable to penetrate the egg coat (Ren *et al.*, 2001), resulting in male infertility (Qi *et al.*, 2007; Quill *et al.*, 2001; Ren *et al.*, 2001). CatSper is essential for fertilization also in humans. Mutations in *CATSPER* genes (Avenarius *et al.*, 2009; Hildebrand *et al.*, 2010) and CatSper dysfunction (Williams *et al.*, 2015) are associated with male infertility. However, mouse and human CatSper channels have distinct properties, indicating that the channel might serve different functions (Kaupp and Strünker, 2016; Alvarez, 2017). For example, in human but not in mouse sperm, CatSper serves as a polymodal sensor that integrates a range of different chemical cues (Brenker *et al.*, 2012; Schiffer *et al.*, 2014; Brenker *et al.*, 2018): human CatSper is activated by **progesterone** and prostaglandins (PGs) (Lishko *et al.*, 2011; Strünker *et al.*, 2011; Brenker *et al.*, 2012), hormones present in the oviductal fluid (Schuetz and Dubin, 1981). The ensuing  $Ca^{2+}$  influx controls the swimming behaviour and promotes the penetration of the egg coat (Schaefer *et al.*, 1998; Harper *et al.*, 2003; Oren-Benaroya *et al.*, 2008; Publicover *et al.*, 2008; Baldi *et al.*, 2009; Kilic *et al.*, 2009; Alasmari *et al.*, 2013a; Schiffer *et al.*, 2014; Tamburrino *et al.*, 2014; Tamburrino *et al.*, 2015). Moreover, progesterone facilitates the migration of human sperm in viscous medium encountered by the sperm during their voyage across the female genital tract (Alasmari *et al.*, 2013b). However, in humans, neither the role of CatSper nor that of progesterone and PGs during fertilization has been fully established. The

function of CatSper in species other than sea urchin, mouse, and human is largely unknown. To address these questions, we rely on pharmacological tools that allow manipulating the function of CatSper.

Several drugs have been identified that suppress CatSper activity, for example, **NNC-0396** (Lishko *et al.*, 2011, Strünker *et al.*, 2011), **mibefradil** (Strünker *et al.*, 2011), MDL12330A (Brenker *et al.*, 2012) and **HC-056456** (Carlson *et al.*, 2009). In patch-clamp experiments, NNC-0396, mibefradil, and MDL12330A abolish CatSper currents (Lishko *et al.*, 2011, Strünker *et al.*, 2011, Brenker *et al.*, 2012); HC-056456 attenuates CatSper currents (Carlson *et al.*, 2009), but it is unknown whether the drug inhibits the channel completely. Of note, none of these drugs is selective for CatSper. The drugs also inhibit the sperm-specific  $K^+$  channel **Slo3 (K<sub>Ca</sub>5.1)** (Navarro *et al.*, 2007; Carlson *et al.*, 2009; Brenker *et al.*, 2014; Mansell *et al.*, 2014), the principal  $K^+$  channel in mouse (Santi *et al.*, 2010; Zeng *et al.*, 2011) and human sperm (Brenker *et al.*, 2014). Notably, each drug inhibits CatSper and Slo3 with similar potency. Moreover, NNC-0396, mibefradil, and MDL12330A exhibit serious adverse actions in human sperm. At the high micromolar concentrations required to abolish  $Ca^{2+}$  influx via CatSper channels, NNC-0396 and mibefradil evoke a sizeable and sustained increase of  $[Ca^{2+}]_i$  and  $pH_i$  (Strünker *et al.*, 2011; Brenker *et al.*, 2012; Chávez *et al.*, 2017) and stimulate acrosomal exocytosis (Chávez *et al.*, 2017; Supporting Information Figure S3). Similarly, MDL12330A at high micromolar concentrations also evokes a sustained  $[Ca^{2+}]_i$  increase in human sperm (Brenker *et al.*, 2012). Finally, the drugs affect the vitality and overall motility of sperm (Tamburrino *et al.*, 2014) (Supporting Information Figure S3). HC-056456 has not been further characterized in human sperm, because it is not commercially available. In conclusion, novel potent and selective CatSper inhibitors without toxic side effects are required.

Before the identification of CatSper channels, the steroidal **sigma receptor** ligand RU1968 was reported to suppress progesterone- and PG-induced  $Ca^{2+}$  signals in human sperm (Schaefer *et al.*, 2000). The mechanism of RU1968 action in sperm has remained unclear, except that it did not involve the activation of sigma receptors (Schaefer *et al.*, 2000). We wondered whether RU1968 might inhibit CatSper and re-examined the actions of this compound in sperm.

Here, we show that RU1968 potently abolishes  $Ca^{2+}$  signals mediated by CatSper in mouse, human, and sea urchin sperm. Patch-clamp recordings from mouse and human sperm confirmed that RU1968 inhibits CatSper. This compound does not affect mouse Slo3 and inhibits human Slo3 channels with about 15-fold lower potency than human CatSper. When present during the capacitation process, RU1968 suppressed hyperactivation in human sperm and inhibited progesterone-evoked motility responses, showing that these effects involve  $Ca^{2+}$  influx via CatSper. Finally, we demonstrate that RU1968 abolishes chemotaxis of sea urchin sperm. In summary, RU1968 is a potent cross-species inhibitor of CatSper channels that is selective for CatSper

over Slo3. This compound seems well-suited to study CatSper channel function in sperm from invertebrates to mammals.

## Methods

### Sperm preparation

The studies involving human sperm were performed in agreement with the standards set by the Declaration of Helsinki. Samples of human semen were obtained from volunteers with their prior written consent. We obtained approval from the institutional ethics committees of the medical association Westfalen-Lippe and the Medical Faculty of the University of Münster (4INie) and from the ethical committee of the University of Birmingham Life and Health Sciences (ERN12-0570R).

For  $\text{Ca}^{2+}$  fluorimetry in sperm populations, single-cell  $\text{Ca}^{2+}$  imaging, patch-clamp recordings, single-cell motility studies and assays for acrosomal exocytosis and viability, sperm were purified by the swim-up procedure in human tubal fluid (HTF) medium containing (in mM): 93.8 NaCl, 4.69 KCl, 0.2  $\text{MgSO}_4$ , 0.37  $\text{KH}_2\text{PO}_4$ , 2.04  $\text{CaCl}_2$ , 0.33 Na-pyruvate, 21.4 lactic acid, 2.78 glucose, 21 HEPES and 4  $\text{NaHCO}_3$ , pH 7.35 (adjusted with NaOH). Sperm were washed and re-suspended in HTF containing 3  $\text{mg}\cdot\text{mL}^{-1}$  human serum albumin (HSA, Irvine Scientific, Santa Ana, CA, USA). For Kremer test, sperm were purified by the swim-up procedure in Supplemented Earle's balanced salt solution (sEBSS), containing (in mM): 98.5 NaCl, 5.4 KCl, 1.8  $\text{CaCl}_2$ , 1  $\text{MgCl}_2$ , 5.5 glucose, 25  $\text{NaHCO}_3$ , 2.5 Na-pyruvate, 19 Na-lactate, 0.81  $\text{MgSO}_4$ , 15 HEPES and 0.3% BSA, pH 7.4 (adjusted with NaOH). Before experiments, sperm were incubated for at least 300 min at 37°C in a 5%  $\text{CO}_2$  atmosphere.

For computer-assisted sperm analysis (CASA), sperm were purified by the swim-up procedure in HTF lacking  $\text{NaHCO}_3$  and HSA. Sperm were washed and re-suspended in this medium (non-capacitating conditions) or in HTF fortified with 25 mM  $\text{NaHCO}_3$  and 3  $\text{mg}\cdot\text{mL}^{-1}$  HSA (capacitating conditions). Before experiments, sperm were incubated for at least 300 min at 37°C and 5%  $\text{CO}_2$  atmosphere.

All animal care and experimental procedures complied with the Guidelines set by the Animal Center of Nanchang University (Approval: SYXK2010-0002) and of the German Animal Welfare Act and the district veterinary office under approval by the LANUV (AZ.02.05.50.16.011 and AZ.84-02.04.2012.A192). Animal studies are reported in compliance with the ARRIVE guidelines (Kilkenny *et al.*, 2010; McGrath and Lilley, 2015). C57BL/6N wild-type (from Janvier, Le Genest-Saint-Isle, France) and C57BL/6N CatSper1<sup>-/-</sup> mice [a kind gift from Prof. David Clapham (Howard Hughes Medical Institute, Janelia Research Campus, USA; Ren *et al.* 2011)] were kept under specific pathogen-free conditions and in ventilated cages (Greenline, Tecniplast). Maximally five mice were housed per cage.

Mouse epididymides were obtained from at least 15-week-old male mice that were anaesthetized with  $\text{CO}_2$  or isoflurane (Abbvie Deutschland, Ludwigshafen, Germany) and killed by cervical dislocation. For patch-clamp recordings, sperm were isolated from the cauda epididymis by swim-out in HS solution containing (in mM): 135 NaCl, 5 KCl, 1  $\text{MgSO}_4$ , 2  $\text{CaCl}_2$ , 20 HEPES, 5 glucose, 10 lactic acid, 1 Na-pyruvate, pH 7.4

(adjusted with NaOH). After 20 min swim-out at 37°C and 10%  $\text{CO}_2$ , the supernatant was collected. Sperm were washed twice and re-suspended in HS solution. For  $\text{Ca}^{2+}$  fluorimetry, sperm were isolated by swim-out in Toyoda, Yokoyama and Hosi (TYH) medium containing (in mM): 138 NaCl, 4.8 KCl, 2  $\text{CaCl}_2$ , 1.2  $\text{KH}_2\text{PO}_4$ , 1  $\text{MgSO}_4$ , 5.6 glucose, 0.5 Na-pyruvate, 10 Na-lactate, 10 HEPES, pH 7.4 (adjusted with NaOH). After 15 min swim-out at 37°C and 5%  $\text{CO}_2$ , sperm were counted and capacitated in TYH-medium supplemented with 25 mM  $\text{NaHCO}_3$  and 3  $\text{mg}\cdot\text{mL}^{-1}$  BSA.

Sperm from the sea urchin *Arbacia punctulata* were obtained by injecting 0.5 M KCl into the body cavity or electrical stimulation of the animal. The ejaculate ('dry sperm') was diluted in artificial sea water (ASW) containing (in mM): 423 NaCl, 9.27  $\text{CaCl}_2$ , 9 KCl, 22.94  $\text{MgCl}_2$ , 25.5  $\text{MgSO}_4$ , 0.1 EDTA, 10 HEPES, pH 7.8 (adjusted with NaOH).

### Measurement of changes in intracellular $\text{Ca}^{2+}$

In human sperm populations, changes in  $[\text{Ca}^{2+}]_i$  and pH<sub>i</sub> were measured with the fluorescent  $\text{Ca}^{2+}$  indicator Fluo4 and BCECF (Thermo Fisher, Waltham, MA, USA), respectively, in 384 multi-well plates in a fluorescence plate reader (Fluostar Omega, BMG Labtech, Ortenberg, Germany) at 29°C, or in a rapid-mixing device in the stopped-flow mode (SFM400, Bio-Logic, Grenoble, France) at 37°C. Sperm were loaded with Fluo4-AM (10  $\mu\text{M}$ ) in the presence of Pluronic F-127 (0.05% w/v) at 37°C for 45 min or with BCECF-AM (10  $\mu\text{M}$ ) at 37°C for 15 min. After incubation, excess dye was removed by centrifugation at 700× *g*, for 10 min, room temperature. Sperm concentration was adjusted to  $5 \times 10^6$  cells·mL<sup>-1</sup> in HTF and equilibrated for 5 min at 29°C (Fluostar) or 37°C (stopped-flow).

In plate-reader experiments, wells were filled with 50  $\mu\text{L}$  of the sperm suspension; the fluorescence was excited at 480 nm (Fluo-4) or 440 and 480 nm (dual excitation, BCECF), and fluorescence emission was recorded at 520 nm. Fluorescence was monitored before and after injection of 25  $\mu\text{L}$  (1:3 dilution) RU1968F1, followed after 5 min by injection of stimuli (1:10 dilution). The solutions were injected into the wells with an electronic multichannel pipette. Changes in Fluo-4 fluorescence are depicted as  $\Delta F/F$  (%), that is, the change in fluorescence ( $\Delta F$ ) relative to the mean basal fluorescence ( $F$ ) before application of buffer or stimuli, to correct for intra- and inter-experimental variations in basal fluorescence among individual wells. Changes in BCECF-fluorescence ratio ( $R$ , 480/440 nm) are depicted as  $\Delta R/R$  (%), that is, the change in ratio ( $\Delta R$ ) relative to the mean basal ratio ( $R$ ) before application of buffer or stimuli, to correct for intra- and inter-experimental variations in the basal fluorescence ratio among individual wells. In stopped-flow experiments, the sperm suspension was rapidly mixed (1:1; flow rate = 1 mL·s<sup>-1</sup>) with HTF containing RU1968F1 and other stimuli, or with K8.6-, KCl-, or pH<sub>8.6</sub>-HTF containing RU1968F1. Fluorescence was excited with a SpectraX Light Engine modulated at 10 kHz (Lumencor, Beaverton, OR, USA) and passed through a 494/20 nm excitation filter (Semrock, Buffalo, NY, USA). Emission was passed through a 536/40 nm filter (Semrock) and recorded with a photomultiplier (H9656-20; Hamamatsu Photonics, Hamamatsu, Japan). Signals were amplified with a lock-in amplifier (7230 DSP, Signal Recovery, Oak Ridge, TN, USA) and recorded with a data acquisition pad (PCI-6221;

National Instruments, Germany) and BioKine software v. 4.49 (Bio-Logic). K8.6-HTF (in mM): 98.5 KCl, 0.2 MgSO<sub>4</sub>, 0.37 KH<sub>2</sub>PO<sub>4</sub>, 2.04 CaCl<sub>2</sub>, 0.33 Na-pyruvate, 21.4 lactic acid, 2.78 glucose, 21 N-[Tris(hydroxymethyl)methyl]-3-aminopropanesulfonic acid (TAPS) and 4 KHCO<sub>3</sub>, pH 8.6 (adjusted with KOH). KCl-HTF (in mM): 98.5 KCl, 0.2 MgSO<sub>4</sub>, 0.37 KH<sub>2</sub>PO<sub>4</sub>, 2.04 CaCl<sub>2</sub>, 0.33 Na-pyruvate, 21.4 lactic acid, 2.78 glucose, 21 HEPES and 4 KHCO<sub>3</sub>, pH 7.35 (adjusted with KOH). pH<sub>o</sub>8.6-HTF (in mM): 93.8 NaCl, 4.69 KCl, 0.2 MgSO<sub>4</sub>, 0.37 KH<sub>2</sub>PO<sub>4</sub>, 2.04 CaCl<sub>2</sub>, 0.33 Na-pyruvate, 21.4 lactic acid, 2.78 glucose, 21 TAPS and 4 NaHCO<sub>3</sub>, pH 8.6 (adjusted with NaOH). Changes in Fluo-4 fluorescence are depicted as ΔF/F (%), that is, the change in fluorescence (ΔF) relative to the fluorescence (F) right after the mixing, to correct for intra- and inter-experimental variations in basal fluorescence. For single-cell Ca<sup>2+</sup> imaging, sperm were incubated in the wells of PLL-coated Greiner Cellview glass slides with Fluo-4-AM (5 μM) for 30 min at 37°C, followed by another 15 min at room temperature to allow settling of sperm on the glass surface. Afterwards, the buffer was replaced twice with 90 μL of 'fresh' HTF to remove excess extracellular dye. Progesterone and RU1968F1 were injected in a 1:10 dilution (10 μL) into the well, and the ensuing changes in [Ca<sup>2+</sup>]<sub>i</sub> were observed under an Olympus IX73 inverted microscope, equipped with a 20×/0.75 objective (U Plan S Apo, Olympus, Germany), coupled to an Andor Zyla 4.2 sCMOS camera (Andor Technology, Belfast, UK). Images were captured at 1 Hz. Changes in [Ca<sup>2+</sup>]<sub>i</sub> were determined from a region of interest around the head and neck of single sperm. Signals are displayed as (F-F<sub>0</sub>)/(F<sub>max</sub>-F<sub>0</sub>); F<sub>0</sub> is the mean fluorescence of ≥5 images before injection of RU1968F1 or progesterone, whereas F<sub>max</sub> is the peak fluorescence signal evoked by a subsequent injection of ionomycin. This procedure corrects for intra- and inter-experimental variations in resting [Ca<sup>2+</sup>]<sub>i</sub> and dye loading among individual sperm.

In mouse sperm populations, changes in [Ca<sup>2+</sup>]<sub>i</sub> were measured in sperm loaded with Cal520-AM (5 μM) (ATT Bioquest, USA) in the presence of Pluronic F-127 (0.02% w/v) for 45 min at 37°C in TYH buffer. After loading, excess dye was removed by three centrifugations (700× g, 7 min, room temperature). Recordings were performed using the stopped-flow apparatus as described above, but with mixing at a flow rate of 0.5 mL·s<sup>-1</sup>. K8.6-TYH (in mM): 4.8 NaCl, 138 KCl, 2 CaCl<sub>2</sub>, 1.2 KH<sub>2</sub>PO<sub>4</sub>, 1 MgSO<sub>4</sub>, 5.6 glucose, 0.5 Na-pyruvate, 10 lactic acid, 10 TAPS, pH 8.6 (adjusted with KOH).

In sea urchin sperm populations, changes in [Ca<sup>2+</sup>]<sub>i</sub> were recorded in Fluo4-loaded sperm. To this end, dry sperm (diluted 1:6 (v/v)) were loaded with Fluo4-AM (10 μM) in the presence of Pluronic F-127 (0.02% w/v) for 45 min at 18°C in ASW. After loading, sperm were diluted 1:20 (v/v) in ASW and allowed to equilibrate for 5 min. Recordings were performed using the stopped-flow apparatus with a flow rate of 1 mL·s<sup>-1</sup>. Fluorescence was excited, recorded, and processed as described above.

KCl-ASW (in mM): 216 KCl, 216 NaCl, 9.27 CaCl<sub>2</sub>, 22.94 MgCl<sub>2</sub>, 25.5 MgSO<sub>4</sub>, 0.1 EDTA, 10 HEPES, pH 7.8, (adjusted with NaOH).

### Patch-clamp recordings

Patch-clamp recordings from human sperm were performed in the whole-cell configuration, as previously described

(Strünker *et al.*, 2011). Seals between pipette and sperm were formed either at the cytoplasmic droplet or the neck region in standard extracellular solution (HS) containing (in mM): 135 NaCl, 5 KCl, 1 MgSO<sub>4</sub>, 2 CaCl<sub>2</sub>, 5 glucose, 1 Na-pyruvate, 10 lactic acid and 20 HEPES, pH 7.4 (adjusted with NaOH). CatSper currents were recorded in divalent-free solutions containing (in mM): 140 CsCl, 40 HEPES, 1 EGTA, pH 7.4 (adjusted with CsOH); the pipette solution contained (in mM): 130 Cs-aspartate, 50 HEPES, 5 EGTA, 5 CsCl, pH 7.3 (adjusted with CsOH). Slo3 currents were recorded in HS with a pipette solution containing (in mM): 140 K-aspartate, 50 HEPES, 10 NaCl, 5 KCl, 0.5 CaCl<sub>2</sub>, pH 7.3 (adjusted with KOH). Currents carried by **H<sub>v</sub>1 channels** were recorded in a bath and pipette solution containing (in mM): 120 NMDG, 100 2-(N-morpholino)ethanesulfonic acid (MES), 5 TEA-Cl, 2 EGTA, pH 6 (adjusted with methanesulfonic acid). To depict mean changes in CatSper currents, CatSper current amplitudes were normalized to that of the monovalent currents in the absence of any progesterone, NH<sub>4</sub>Cl or RU1068F1. This procedure corrects for variations in amplitudes among individual sperm to ease and to improve the clarity of the graphical illustration. Patch-clamp recordings from mouse sperm were performed in the whole-cell configuration, as previously described (Kirichok *et al.*, 2006; Zeng *et al.*, 2011). Seals between pipette and sperm were formed at the cytoplasmic droplet. For Slo3 recordings, the extracellular solution contained (in mM): 160 KOH, 10 HEPES, 150 MES and 2 Ca(MES)<sub>2</sub>, adjusted to pH 7.4 with MES; the pipette solution contained (in mM): 155 KOH, 5 KCl, 10 BAPTA, 20 HEPES, 115 MES, pH 8.0 (adjusted with KOH). CatSper currents were recorded in divalent-free solutions containing (in mM): 150 NaCl, 20 HEPES, 5 EDTA, pH 7.4 (adjusted with NaOH); and with a pipette solution containing (in mM) 135 Cs-MES, 10 HEPES, 10 EGTA and 5 CsCl, pH 7.2 (adjusted with CsOH). Current amplitudes were normalized to that of the monovalent currents in the absence of NH<sub>4</sub>Cl or RU1968F1 (control) to correct for variations in amplitudes among individual sperm.

Human T-type (**Ca<sub>v</sub>3.2**) and L-type (**Ca<sub>v</sub>1.2** + β2b + α2δ1) Ca<sup>2+</sup> channels were studied in HEK293T cells (The European Collection of Cell Cultures, Porton Down, UK) that were cultured according to the supplier's protocol in the presence of penicillin G (100 U·mL<sup>-1</sup>) and streptomycin (10 mg·mL<sup>-1</sup>). Cells were transfected at 40% confluency with pcDNA3.1-CACNA1C, pcDNA3.1-CaVb2b and pIRES-dsRed-CaVa2d1 in a ratio of 2:1:1 μg, or with 2 μg of pCMV-Entry-CACNA1H, using the calcium-phosphate precipitation method. Patch-clamp recordings from HEK293T cells were performed in the whole-cell configuration, using a HEKA EPC 10 amplifier with PatchMaster software (both HEKA Elektronik, Lambrecht, Germany). The extracellular solution contained (in mM): 125 TEA-Cl, 15 glucose, 10 HEPES, 5 CaCl<sub>2</sub>, pH 7.4, (adjusted with CsOH); the pipette solution contained (in mM): 100 CsCl, 10 EGTA, 10 HEPES, 5 TEA-Cl, 5 MgATP, 0.2 NaGTP, pH 7.4 (adjusted with CsOH). RU1968F1 was applied via a gravity-driven perfusion system.

### Analysis of sperm motility

To evaluate the acute action of RU1968F1 on motility parameters, sperm from a particular sample were incubated side-by-side in HTF lacking NaHCO<sub>3</sub> and HSA (non-capacitating medium) and in capacitating medium (25 mM NaHCO<sub>3</sub>/

3 mg·mL<sup>-1</sup> HSA). After 3 h of incubation at 37°C, sperm kinematic parameters were analysed by a CASA system (CEROS, Hamilton Thorn Research, Beverly, MA, USA) before and after application of RU1968F1. Sperm were bathed in RU1968F1 for 5 min prior to the experiment. To evaluate the long-term action of RU1968F1 on sperm motility parameters, sperm were re-suspended in capacitating medium (HTF containing 25 mM NaHCO<sub>3</sub> and 3 mg·mL<sup>-1</sup> HSA) with or without RU1968F1. After 3 h of incubation at 37°C, sperm kinematic parameters were analysed by CASA. To evaluate the action of RU1968F1 on progesterone-induced hyperactivation, capacitated sperm were incubated for 5 min in the absence (control) and presence of progesterone, RU1968F1, and progesterone plus RU1968F1, and the motility was analysed by CASA. The following parameters were determined by CASA: curvilinear velocity (VCL,  $\mu\text{m}\cdot\text{s}^{-1}$ ), amplitude of lateral head displacement (ALH,  $\mu\text{m}$ ), linearity of progression (LIN, %), percentage of total, progressive and rapid motility as well as percentage of motile, hyperactivated sperm. The threshold values for hyperactivation were manually set (VCL > 150  $\mu\text{m}\cdot\text{s}^{-1}$ , ALH > 7  $\mu\text{m}$ , LIN < 50% (Mortimer *et al.*, 1998; Tamburrino *et al.*, 2014). A minimum of 100 cells and five fields of view were analysed for each aliquot. The experiments were performed at 37°C.

Motility in human sperm evoked by uncaging of progesterone were studied in an observation chamber (100  $\mu\text{m}$  depth) under an Olympus IX71 inverted microscope (Olympus, Tokyo, Japan), equipped with a 4 $\times$  microscope objective (0.13 NA, UPLFLN-PH, Olympus) under dark-field illumination [red light-emitting diode (LED), M660 L3-C1, Thorlabs]. Movies were recorded at a total magnification of 6.4 $\times$  with a high-speed CMOS camera (Dimax HD, PCO, Kelheim, Germany) at 150 Hz. Photolysis of caged progesterone (1  $\mu\text{M}$ ) (Kilic *et al.*, 2009) was achieved using a 200 ms light flash delivered by a 365 nm LED (M365 L2-C, Thorlabs, Munich, Germany). Movies were processed and analysed using a customized CASA plugin for ImageJ. Changes in the velocity average path (VAP) are shown as VAP (%), that is, the change in VAP relative to the VAP right before the UV flash, to correct for intra- and inter-experimental variations and for the different resting VAP in the absence and presence of the inhibitor. This procedure eases and improves the clarity of the graphical illustration.

Kremer penetration assays were performed in sEBSS supplemented with methylcellulose (1% w/v) and 0.3% BSA, equilibrated overnight at 4°C (penetration medium). The penetration medium, with or without RU1968F1, was filled into flattened glass capillary tubes (dimensions: 1.2  $\times$  4.8  $\times$  50 mm, 400  $\mu\text{m}$  depth; CM scientific, UK); one end of the tubes was sealed with CristaSeal wax (Hawksley, UK). The open ends of the tubes were submerged in a sperm suspension (3  $\times$  10<sup>6</sup>·mL<sup>-1</sup>) with or without stimuli and/or RU1968F1. Penetration was assessed after 1 h (37°C, 5.5% CO<sub>2</sub>) by counting sperm at 2 cm using a phase contrast microscope at a 200 $\times$  magnification. Three fields of view were chosen, and in each field, three focal planes were counted, yielding nine fields altogether.

Human sperm viability and motility, as shown in Supporting Information Figure S3, was tested following incubation of sperm for 5 min at room temperature with RU1968F1, NNC-55-0396, mibefradil or the vehicle (DMSO). The fraction of immotile and dead sperm was assessed by

counting and by an eosin vitality test, respectively, at 200 $\times$  magnification under a phase-contrast microscope (Axiostar, Carl Zeiss), in accordance with the WHO guidelines for semen analysis (WHO, 2010). For the eosin staining, 5  $\mu\text{L}$  of the sperm suspension was mixed with 5  $\mu\text{L}$  of eosin staining solution [0.5% (w/v) eosin Y dissolved in a 0.9% NaCl solution] on a microscope slide, covered with a 22  $\times$  22 mm coverslip and incubated for 30 s at RT. Eosin-positive (dead) versus eosin-negative (live) sperm were counted. To determine the fraction of immotile and viable sperm, a total number of 400 sperm were assessed.

Sea urchin sperm chemotaxis was studied as described (Seifert *et al.*, 2015). In brief, sperm ( $\sim 10^8$  cells·mL<sup>-1</sup>) were observed in a recording chamber (150  $\mu\text{m}$  depth) under an IX71 microscope (Olympus), equipped with a 10 $\times$  microscope objective (UPlanSApo; NA 0.4; Olympus), with stroboscopic (500 Hz) dark-field illumination (white LED; K2 star; Luxeon). Movies were recorded with an EMCCD camera (DU-897D; Andor) at 20 Hz through a bandpass filter (HQ520/40; Chroma). Photolysis of caged resact was achieved using a 200 ms pulse from a 365 nm LED (M365 L2-C, Thorlabs). The relative dispersion was calculated as described before (Seifert *et al.*, 2015).

### Acrosomal exocytosis

Human sperm, capacitated for at least 300 min, were incubated with either 0.1% DMSO (vehicle control), RU1968F1 (10  $\mu\text{M}$ ), progesterone (10  $\mu\text{M}$ ) or a mixture of both (10  $\mu\text{M}$  each) for 1 h at 37°C. Afterwards, sperm were washed by centrifugation and re-suspended in 0.5 mL of hypo-osmotic swelling medium (WHO, 2010). After 1 h at 37°C, sperm were washed again and fixed in 50  $\mu\text{L}$  ice-cold methanol. The sperm were layered on a slide, air-dried, and stored at -20°C. For acrosome staining, sperm were incubated for 20 min in the dark with 1 mg·mL<sup>-1</sup> FITC-labelled *Arachis hypogaea* (peanut) lectin (PNA-FITC, Sigma Aldrich) in PBS. Slides were analysed using an Axiolab A1 FL microscope (Carl Zeiss, Jena, Germany). For each condition, 200 curled-tail (viable) cells were analysed for their acrosomal status, as previously described (Tamburrino *et al.*, 2014).

### Data analysis and statistical evaluation

The data and statistical analysis comply with the recommendations on experimental design and analysis in pharmacology (Curtis *et al.*, 2018). Experiments and data analysis were performed without randomization and blinding, except for the Eosin test and the manual counting of motile/immotile sperm. Otherwise, non-treated and treated conditions were measured and analysed side-by-side by the same experimenter, using objective measures and analysis methods.

All data are presented as mean  $\pm$  SD. Statistical analysis and fitting of dose-response relations were performed using GraphPad Prism 5 (Prism, La Jolla, USA). Half-maximal inhibitory concentrations (IC<sub>50</sub>) were derived by nonlinear regression analysis, using a four parameter fit:

$$Y = \text{bottom} + \frac{(\text{top} - \text{bottom})}{\left(1 + 10^{(\log(\text{IC}_{50} - x)/n)}\right)}$$

Y = signal amplitude; bottom and top = plateaus in the units of Y; x = log(concentration of inhibitor); IC<sub>50</sub> = concentration

of agonist that gives the response half way between bottom and top;  $n$  = Hill coefficient.

Most of the experiments were performed in a randomized block design, that is, for each experimental replicate, sperm prepared from one particular semen sample were subjected in parallel to all treatment conditions. If the experiment involved two conditions (control and treatment), we used the paired *t*-test. If the experiment involved  $\geq 3$  conditions, we used one-way randomized block ANOVA, assuming sphericity. When ANOVA's F-test and the test for matching efficacy achieved  $P < 0.05$ , means were compared to the control's mean by Dunnett's multiple comparisons *post hoc* test, unless otherwise indicated. If experiments were not performed in a randomized block design, we used unpaired *t*-test or one-way ANOVA; when ANOVA's F-test achieved  $P < 0.05$  and Bartlett's test yielded no significant variance inhomogeneity, means were compared to the control's mean or to each other by Dunnett's or Bonferroni's multiple comparisons *post hoc* test respectively. In Figures 6E, J, and 8I, for the ease of illustration and for clarity, we show data normalized to the control. We normalized the data only after the statistical analysis using one-way ANOVA, because normalization makes any data set violate the ANOVA.

## Materials

The suppliers of the compounds used in these experiments are as follows: progesterone from Sigma and the caged form was prepared as described by Kilic *et al.*, 2009; 8-Br-cAMP was from BioLog (Bremen, Germany); resact and its caged form were prepared as described by Böhmer *et al.*, 2005 and Kaupp *et al.*, 2003; mibefradil, MDL12330A, NNC-0396 and PGE<sub>1</sub> were supplied by Tocris (Wiesbaden-Nordenstadt, Germany).

## Nomenclature of targets and ligands

Key protein targets and ligands in this article are hyperlinked to corresponding entries in <http://www.guidetopharmacology.org>, the common portal for data from the IUPHAR/BPS Guide to PHARMACOLOGY (Harding *et al.*, 2018), and are permanently archived in the Concise Guide to PHARMACOLOGY 2017/18 (Alexander *et al.*, 2017a,b).

guidetopharmacology.org, the common portal for data from the IUPHAR/BPS Guide to PHARMACOLOGY (Harding *et al.*, 2018), and are permanently archived in the Concise Guide to PHARMACOLOGY 2017/18 (Alexander *et al.*, 2017a,b).

## Results

### Synthesis of RU1968

We synthesized RU1968 from ( $\pm$ ) estrone methyl ether (Figure 1A and Supporting Information Figure S1) that is readily accessible via the Torgov route (Ananchenko *et al.*, 1962; Ananchenko and Torgov, 1963). Van Leusen reaction yielded the nitrile (1) (Van Leusen and Van Leusen, 2004), followed by addition of methyllithium to yield the ketone (2). Reductive amination with *N,N*-dimethylethylenediamine established the aza side chain, yielding a mixture of four diastereomers (3) (at C-17 and C-20; Figures 1A compound 3). We separated two diastereomers (Figure 1A, compounds 3a and 3b), each a mixture of a *cis* and a *trans* isomer. Relative configurations [C-18 (CH<sub>3</sub>) and C-20 (CH)] were assigned by NMR spectroscopy (H,H-COSY and NOE, Supporting Information Figures S1 and S2); the *cis* isomers were the dominant species (*cis/trans* ratio for compound 3a was 3:1; and for 3b, it was 4:1). Finally, cleavage of the phenolic methyl ether yielded a diastereomeric mixture of RU1968. The diastereomers eluted from a preparative HPLC in four fractions called RU1968F1-4; RU1968F1 and 2 are derived from 3a *cis* and *trans*, respectively, whereas RU1968F3 and 4 are derived from 3b *trans* and *cis*, respectively (Figure 1C). Because the actions of RU1968F2-4 in sperm were similar to that of RU1968F1 (see Figure 2 and Supporting Information Figures S3 and S6), we chose RU1968F1 to characterize its action in sperm. We first examined the action of RU1968F1 in populations of human sperm loaded with a fluorescent pHi or Ca<sup>2+</sup> indicator

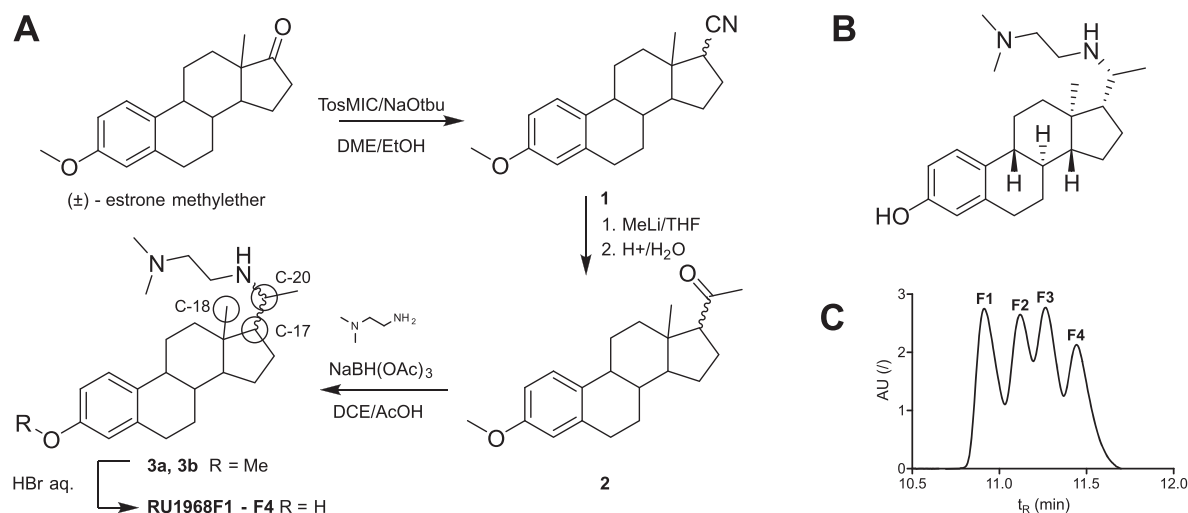


**Figure 1**

Synthesis of RU1968F1-F4. (A) Synthesis of RU1968. Carbon atoms referred to in the text are marked with circles. (B) Structure of RU1968. (C) HPLC-elution profile of the four diastereomers. Isomers are named according to their order of elution.

(Supporting Information Figure S3A–D). The drug evoked negligible changes in  $pH_i$ . At concentrations  $\leq 7.5 \mu\text{M}$ , RU1968F1 caused a small, transient  $\text{Ca}^{2+}$  increase;  $[\text{Ca}^{2+}]_i$  peaked and returned to basal levels within about 250 s. At concentrations  $>7.5 \mu\text{M}$ , RU1968F1 evoked a slow decrease of  $[\text{Ca}^{2+}]_i$ . The mechanism(s) underlying the drug-evoked changes in  $[\text{Ca}^{2+}]_i$  are unclear. In the absence of extracellular  $\text{Ca}^{2+}$ , the drug did not change  $[\text{Ca}^{2+}]_i$ , indicating that  $\text{Ca}^{2+}$  release from internal stores is not involved (Supporting Information Figure S3C). Most importantly, even at high micromolar concentrations (30  $\mu\text{M}$ ), the drug did not affect overall human sperm motility and viability and did not evoke acrosomal exocytosis (Supporting Information Figure S3E–G). Thus, RU1968F1 lacks the toxic and adverse actions of NNC-0396, mibefradil, and MDL12330A in human sperm.

### RU1968F1 is a potent cross-species inhibitor of CatSper channels

To investigate whether RU1968F1 inhibits human CatSper channels, we studied progesterone- and  $\text{PGE}_1$ -evoked  $\text{Ca}^{2+}$  signals in human sperm in the presence of RU1968F1. RU1968F1 slowed down and completely suppressed the  $\text{Ca}^{2+}$  signals in a dose-dependent fashion. The  $\text{IC}_{50}$  values of  $4 \pm 2 \mu\text{M}$  (progesterone) and  $3.8 \pm 0.5 \mu\text{M}$  ( $\text{PGE}_1$ ) ( $n = 7$ , mean  $\pm$  SD) were similar to those reported previously (Schaefer *et al.*, 2000) (Figure 2A–D). The compound was effective within a range of extracellular pH ( $pH_o$ ) values: at  $pH_o$  6.8 and 7.8, the  $\text{IC}_{50}$  value of the progesterone-evoked  $\text{Ca}^{2+}$  signal was  $4.4 \pm 1.4$  and  $2.2 \pm 0.6 \mu\text{M}$ , respectively ( $n = 6$ ) (Figure 2B). The actions of RU1968F2-4 alone and on progesterone-evoked  $\text{Ca}^{2+}$  signals were similar to those of RU1968F1 (see Figure 2 and Supporting Information Figures S3 and S6).

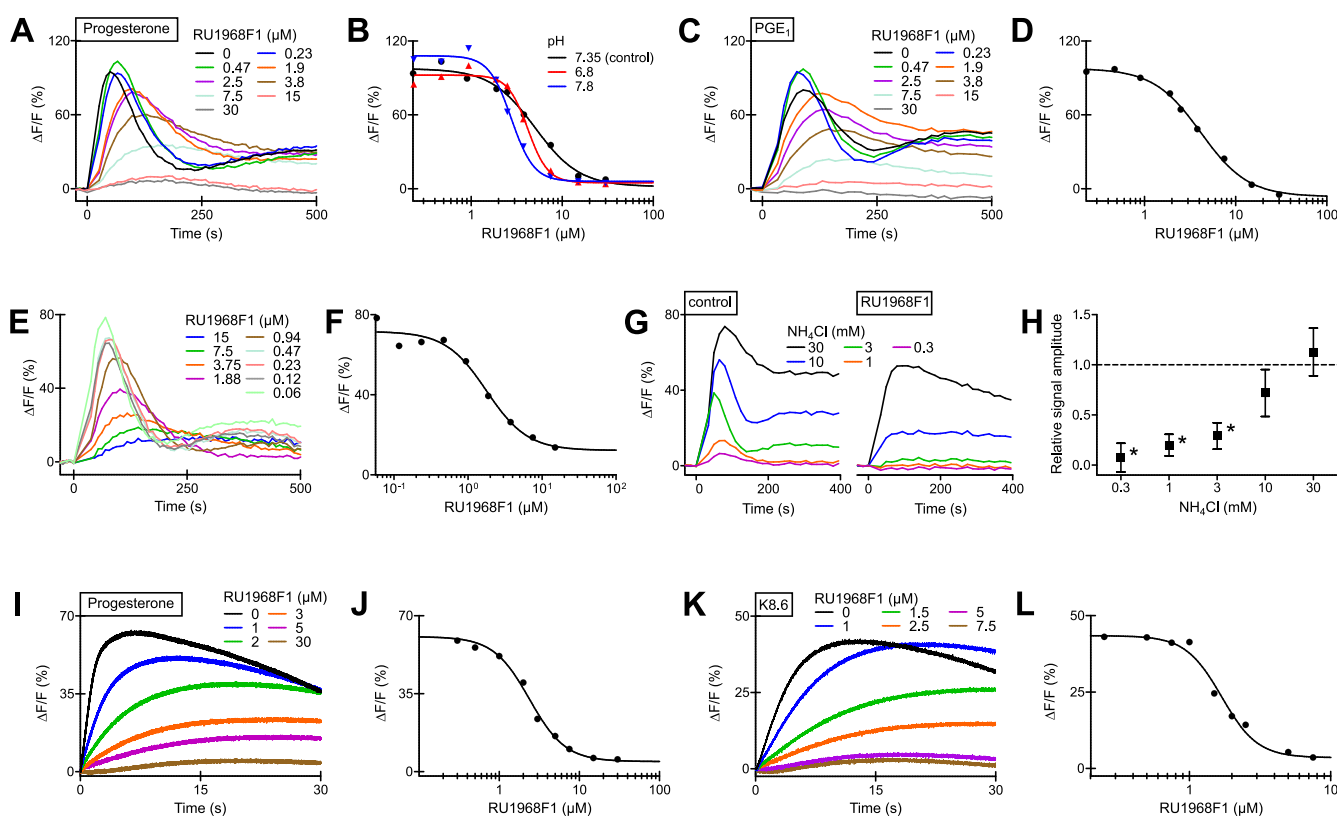


**Figure 2**

Action of RU1968F1 on CatSper-mediated  $\text{Ca}^{2+}$  signals in human sperm populations. (A) Progesterone-evoked  $\text{Ca}^{2+}$  signals in human sperm in the absence and presence of RU1968F1.  $\Delta\text{F}/\text{F}$  (%) indicates the percentage change in fluorescence ( $\Delta\text{F}$ ) with respect to the mean basal fluorescence (F) before application of progesterone (500 nM). (B) Dose–response relation for the maximal signal amplitudes of the data from (A) ( $pH$  7.35) ( $\text{IC}_{50} = 5.5 \mu\text{M}$ ) and of progesterone responses studied at an extracellular  $pH$  of 6.8 ( $\text{IC}_{50} = 4.2 \mu\text{M}$ ) or 7.8 ( $\text{IC}_{50} = 2.6 \mu\text{M}$ ). (C)  $\text{PGE}_1$ -evoked  $\text{Ca}^{2+}$  signals in human sperm in the absence and presence of RU1968F1;  $\text{PGE}_1 = 500 \text{ nM}$ . (D) Dose–response relation for the maximal signal amplitudes of the data from (C) ( $\text{IC}_{50} = 3.1 \mu\text{M}$ ). (E)  $\text{NH}_4\text{Cl}$ -evoked  $\text{Ca}^{2+}$  signals in the absence and presence of RU1968F1,  $\text{NH}_4\text{Cl} = 3 \text{ mM}$ . (F) Dose–response relation for the maximal signal amplitude of the data from (E) ( $\text{IC}_{50} = 1.8 \mu\text{M}$ ) (G)  $\text{Ca}^{2+}$  signals evoked by various  $\text{NH}_4\text{Cl}$  concentrations in the absence (control) and presence of RU1968F1 (30  $\mu\text{M}$ ). (H) Mean relative amplitude of  $\text{Ca}^{2+}$  signals evoked by various  $\text{NH}_4\text{Cl}$  concentrations in the presence of RU1968F1 (30  $\mu\text{M}$ ) ( $n = 5$ ); amplitude evoked in the absence of RU1968F1 = 1 (control). Data shown are means  $\pm$  SD. \* $P < 0.05$ , significantly different from control. (I)  $\text{Ca}^{2+}$  signals evoked by simultaneous mixing of sperm with progesterone (500 nM) and RU1968F1 in a stopped-flow apparatus.  $\Delta\text{F}/\text{F}$  (%) indicates the percentage change in fluorescence ( $\Delta\text{F}$ ) with respect to the fluorescence (F) immediately after mixing. (J) Dose–response relation of the data from (I) ( $\text{IC}_{50} = 2.4 \mu\text{M}$ ). (K)  $\text{Ca}^{2+}$  signals evoked by mixing of sperm with K8.6-HTF and RU1968F1. The final  $\text{K}^+$  concentration and  $pH$  after mixing was 51.25 mM and 8.1 respectively. (L) Dose–response relation of the data from (K) ( $\text{IC}_{50} = 1.7 \mu\text{M}$ ).

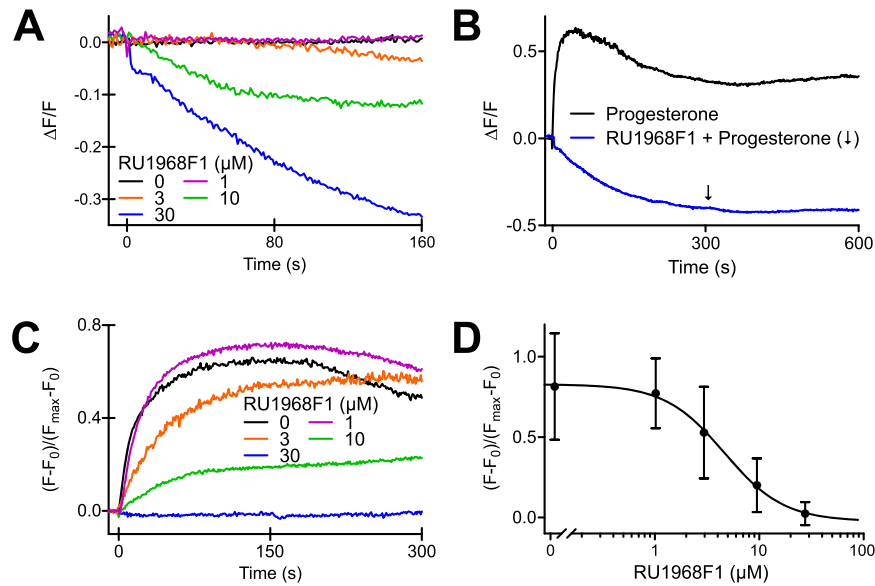


### Figure 3

Action of RU1968F1 on progesterone-evoked  $\text{Ca}^{2+}$  signals in single human sperm. (A) Changes in  $[\text{Ca}^{2+}]_i$  evoked by RU1968F1 in immobilized sperm. Sperm were challenged with RU1968F1 at  $t = 0$ . Traces represent averages of 122 (RU1968F1, 0  $\mu\text{M}$ ), 344 (1  $\mu\text{M}$ ), 42, (3  $\mu\text{M}$ ), 165 (10  $\mu\text{M}$ ) and 109 (30  $\mu\text{M}$ ) sperm from three donors. Signals are displayed as  $(F-F_0)/(F_{\text{max}}-F_0)$ ;  $F_0$  is the mean fluorescence of  $\geq 5$  images before application of RU1968F1;  $F_{\text{max}}$  is the peak fluorescence signal evoked by ionomycin (not shown) to gauge the maximal response amplitude. (B) Progesterone-evoked  $\text{Ca}^{2+}$  responses (2  $\mu\text{M}$ ) in the absence and presence of RU1968F1 (30  $\mu\text{M}$ ); averages of 50 (control) and 109 (RU1968F1) sperm from three donors. Progesterone and RU1968F1 were applied at  $t = 0$ ; following application of RU1968F1, progesterone was applied at the time point indicated by the arrow. (C) Amplitude of progesterone-evoked  $\text{Ca}^{2+}$  responses in the absence and presence of different RU1968F1 concentrations; averages of 122 (RU1968F1, 0  $\mu\text{M}$ ), 344 (1  $\mu\text{M}$ ), 42 (3  $\mu\text{M}$ ), 165 (10  $\mu\text{M}$ ) and 109 (30  $\mu\text{M}$ ) sperm from three donors. (D) Mean amplitude of progesterone-evoked  $\text{Ca}^{2+}$  signals (2  $\mu\text{M}$ ) in the presence of RU1968F1; number of sperm: 310 (RU1968F1, 0  $\mu\text{M}$ ), 552 (1  $\mu\text{M}$ ), 181 (3  $\mu\text{M}$ ), 302 (10  $\mu\text{M}$ ) and 222 (30  $\mu\text{M}$ ). Data shown are means  $\pm$  SD. Fitting of a dose–response curve to the data yielded an  $\text{IC}_{50}$  of  $4.8 \pm 1.2$   $\mu\text{M}$  (standard error of the fit).

Furthermore, we studied whether RU1968F1 also inhibits  $\text{Ca}^{2+}$  signals evoked by intracellular alkalization via the weak base  $\text{NH}_4\text{Cl}$  (Figure 2E–H). The compound slowed down and almost completely suppressed  $\text{Ca}^{2+}$  signals evoked by  $\text{NH}_4\text{Cl} \leq 3$  mM (Figure 2E, F); the  $\text{IC}_{50}$  value for 3 mM  $\text{NH}_4\text{Cl}$  was  $4.0 \pm 2.8$   $\mu\text{M}$  ( $n = 5$ ) (Figure 2F, G).  $\text{Ca}^{2+}$  signals evoked by 10 mM  $\text{NH}_4\text{Cl}$  were only slightly attenuated, whereas for 30 mM  $\text{NH}_4\text{Cl}$ , the signal was rather similar in the absence and presence of RU1968F1 (Figure 2G, H). We conclude that RU1968F1 inhibits also  $\Delta\text{pH}_i$ -evoked  $\text{Ca}^{2+}$  responses. However, its potency seems to decrease with increasing  $\Delta\text{pH}_i$ . Alternatively, the presence of  $\text{NH}_4^+$  or  $\text{NH}_3$  might impair binding of RU1968F1 to its blocking site. Arguing against that notion, the compound readily suppressed progesterone responses in sperm that were bathed for about 20 min in  $\text{NH}_4\text{Cl}$  (30 mM) (Supporting Information Figure S5;  $\text{IC}_{50} = 3.5 \pm 1.4$   $\mu\text{M}$ ,  $n = 3$ ); with time, the  $\text{pH}_i$  slowly recovers from the  $\text{NH}_4\text{Cl}$ -evoked alkalization (Strünker *et al.*, 2011).

Influx of  $\text{Ca}^{2+}$  via CatSper can also be evoked by simultaneous extracellular alkalization (which increases  $\text{pH}_e$ ) and depolarization by  $\text{K}^+$  (K8.6 buffer) (see Carlson *et al.*, 2003). RU1968F1 suppressed  $\text{Ca}^{2+}$  signals evoked by simultaneous alkalization/depolarization (Figure 2K, L;  $\text{IC}_{50} = 1.2 \pm 0.6$   $\mu\text{M}$ ,  $n = 3$ ) and by alkalization or depolarization alone (Supporting Information Figure S4). Finally, when sperm were mixed simultaneously with progesterone and RU1968F1 in a stopped-flow

apparatus, the inhibition of  $\text{Ca}^{2+}$  responses was similar to that under pre-incubation conditions (Figure 2I, J) ( $\text{IC}_{50} = 3.0 \pm 1.1$   $\mu\text{M}$ ;  $n = 4$ ). This result suggests that RU1968F1 rapidly reaches its blocking site.

Next, we studied the action of RU1968F1 in single human sperm by  $\text{Ca}^{2+}$  imaging. At concentrations  $\geq 10$   $\mu\text{M}$ , RU1968F1 evoked a slow decrease of  $[\text{Ca}^{2+}]_i$  (Figure 3A). For low micromolar RU1968F1 concentrations, we did not observe  $\text{Ca}^{2+}$  transients, which might reflect differences in sensitivity of population versus single-cell fluorimetry. In the presence of RU1968F1, progesterone-induced  $\text{Ca}^{2+}$  responses were suppressed in a dose-dependent fashion (Figure 3B–D) with an  $\text{IC}_{50}$  of  $4.8 \pm 1.2$   $\mu\text{M}$  (standard error of the fit). Altogether, the action of the RU1968F1 itself on  $[\text{Ca}^{2+}]_i$  and on progesterone-evoked  $\text{Ca}^{2+}$  responses is similar when investigated in sperm populations and in single sperm.

We further tested whether the compound also inhibited  $\text{Ca}^{2+}$  influx via CatSper channels in mouse sperm. Mouse CatSper is insensitive to progesterone and PGs (Lishko *et al.*, 2011). Therefore, we activated CatSper via simultaneous alkalization/depolarization or via 8-Br-cAMP, which activates mouse (Ren *et al.*, 2001) and human (Brenker *et al.*, 2012) CatSper at high concentrations. RU1968F1 suppressed  $\text{Ca}^{2+}$  responses evoked by alkalization/depolarization or 8-Br-cAMP with an  $\text{IC}_{50}$  of  $0.83 \pm 0.07$  and  $0.84 \pm 0.03$   $\mu\text{M}$  respectively ( $n = 3$ ) (Figure 4A–D).



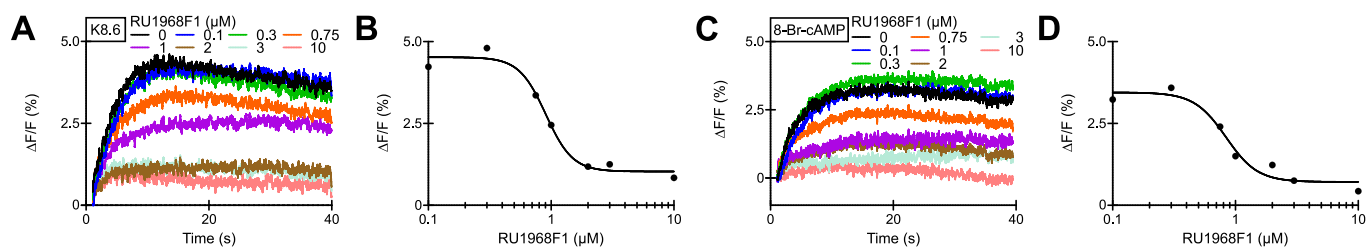


**Figure 4**

Action of RU1968F1 on CatSper-mediated  $\text{Ca}^{2+}$  signals in mouse sperm populations. (A)  $\text{Ca}^{2+}$  signals evoked by simultaneous mixing of mouse sperm with K8.6-TYH and RU1968F1 in a stopped-flow apparatus. After mixing, the final  $\text{K}^+$  concentration and pH was 69 mM and 8.1 respectively. (B) Dose–response relation of the data from (A) ( $\text{IC}_{50} = 0.90 \mu\text{M}$ ). (C)  $\text{Ca}^{2+}$  signals evoked by simultaneous mixing of mouse sperm with 8-Br-cAMP (20 mM) and RU1968F1. (D) Dose–response relation of the data from (C) ( $\text{IC}_{50} = 0.84 \mu\text{M}$ ).

Finally, we investigated the action of RU1968F1 on CatSper in sperm of the sea urchin *A. punctulata*. To this end, we studied CatSper-mediated  $\text{Ca}^{2+}$  responses evoked either by the chemoattractant resact, depolarization of  $V_m$ , or by  $\text{NH}_4\text{Cl}$ . Irrespective of the stimulus, RU1968F1 suppressed the  $\text{Ca}^{2+}$  responses with  $\text{IC}_{50}$  values of  $1.3 \pm 0.1$ ,  $1.1 \pm 0.4$  and  $4 \pm 2$  respectively ( $n = 3$ ) (Figure 5A–F). Altogether, these results suggest that RU1968F1 is a potent cross-species CatSper inhibitor.

To scrutinize this conclusion by an independent technique, we recorded CatSper currents in human and mouse sperm by whole-cell patch clamping. In human sperm, monovalent CatSper currents were evoked by stepping the membrane voltage from  $-100$  to  $+150$  mV in increments of 10 mV from a holding potential of 0 mV. RU1968F1 completely suppressed these currents with an  $\text{IC}_{50}$  of  $0.4 \pm 0.3 \mu\text{M}$  ( $n = 5$ ) (Figure 6A, B). Superfusion with progesterone or  $\text{NH}_4\text{Cl}$  enhanced the current amplitudes (Figure 6C, D). The progesterone- and  $\text{NH}_4\text{Cl}$ -evoked currents were either completely suppressed or strongly attenuated by RU1968F1 (Figure 6C–E). In mouse sperm, monovalent CatSper currents were evoked by ramping the membrane voltage between  $-100$  and  $+100$  mV from a holding potential of 0 mV. Superfusion with RU1968F1 completely suppressed the currents with an  $\text{IC}_{50}$  of  $10 \pm 1 \mu\text{M}$  (Figure 6F, G). CatSper currents evoked at  $\text{pH}_i$  8 and by  $\text{NH}_4\text{Cl}$  were strongly attenuated by the drug (Figure 6H–J). Thus, RU1968F1 inhibits human and mouse CatSper at rest and upon activation by ligands and  $\Delta\text{pH}_i$ . Similar to the results obtained by  $\text{Ca}^{2+}$  fluorimetry, the potency of the drug decreased with increasing  $\text{pH}_i$ . We did not test whether higher RU1968F1 concentrations completely suppress the currents evoked by  $\text{NH}_4\text{Cl}$  and at  $\text{pH}_i$  8.

### RU1968F1 inhibits human but not mouse Slo3 channels

We studied the interaction of RU1968F1 with sperm ion channels other than CatSper. In mouse sperm, currents carried by the  $\text{K}^+$  channel Slo3 were similar in the absence and presence of RU1968F1 (Figure 7A, B). By contrast, in human sperm, the Slo3 current was inhibited with an  $\text{IC}_{50}$  of  $7 \pm 6 \mu\text{M}$  ( $n = 4$ ) (Figure 7C, D). Thus, although not completely selective for CatSper, about 15-fold higher RU1968F1 concentrations were required to block human Slo3. At concentrations up to  $10 \mu\text{M}$ , the compound did not inhibit the

voltage-gated proton channel  $\text{H}_v1$  and the ATP-gated **P2X channel** (Supporting Information Figure S7), which are expressed in human and mouse sperm, respectively (Lishko *et al.*, 2010; Navarro *et al.*, 2011). We conclude that in mouse sperm, RU1968F1 acts rather selectively on CatSper. In human sperm, the compound also inhibited Slo3, but with about 15-fold lower potency. Finally, RU1968F1 inhibited heterologously expressed L- and T-type  $\text{Ca}^{2+}$  channels with  $\text{IC}_{50}$  values of about 20 and  $10 \mu\text{M}$ , respectively (Supporting Information Figures S9 and S10), indicating that the compound also acts with lower potency on classic voltage-gated  $\text{Ca}^{2+}$  channels of somatic cells.

### RU1968F1 suppresses progesterone-evoked motility responses in human sperm

Next, we tested the action of RU1968F1 on the motility of human sperm using CASA. A brief incubation (5 min) of non-capacitated or capacitated sperm with the compound did not impair overall motility (Figure 8A, B), whereas the fraction of progressively motile sperm decreased about twofold with increasing RU1968F1 concentrations (Figure 8A, B). Whether this is due to the inhibition of CatSper channels or represents an adverse action of the drug is unclear.

Furthermore, the penetration of the egg coat requires hyperactivated motility, which is characterized by an asymmetric flagellar beat, lower beating frequency, wiggly swimming trajectory and lower VAP (Suarez, 2008). In mouse sperm, CatSper channels are required for hyperactivation (Ren *et al.*, 2001), whereas the control of hyperactivation by CatSper in human sperm is debated (Alasmari *et al.*, 2013b; Tamburrino *et al.*, 2014). We studied whether RU1968F1 affects hyperactivation in human sperm. A brief incubation (5 min) of capacitated sperm with RU1968F1 did not suppress spontaneous hyperactivated swimming. In fact, RU1968F1 concentrations  $<10 \mu\text{M}$  seem to slightly enhance hyperactivation, whereas higher concentrations had no effect (Figure 8B). Spontaneous hyperactivation develops during the capacitation process (compare Figure 8A, B). In sperm that were capacitated in the presence of RU1968F1 ( $10 \mu\text{M}$ ), that is, incubated for some hours under capacitating conditions, the compound suppressed spontaneous hyperactivation (Figure 8C), while the fraction of progressively motile sperm or overall motility was not affected (Figure 8D, E). This result suggests that, in human sperm, CatSper channels are involved in the ability to undergo hyperactivation; though,

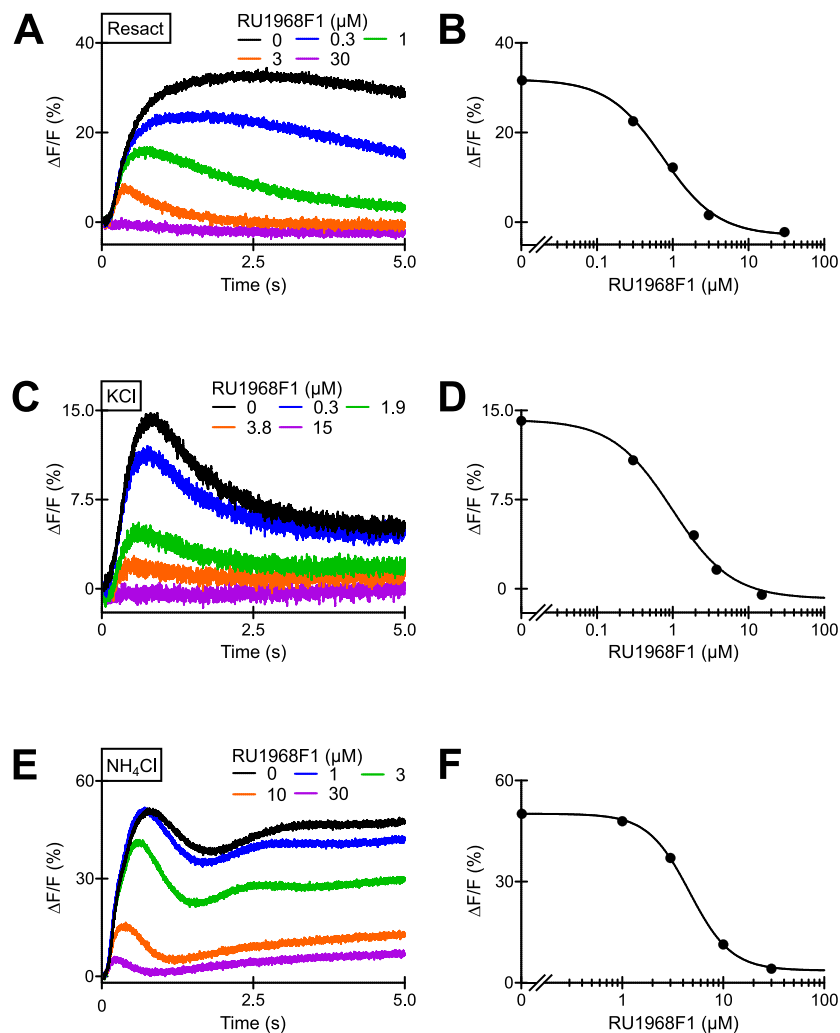


### Figure 5

Action of RU1968F1 on  $\text{Ca}^{2+}$  responses mediated by CatSper channels in sea urchin sperm. (A) Resact-induced  $\text{Ca}^{2+}$  signals in sea urchin sperm evoked by simultaneous mixing of sperm with resact (20 pM) and RU1968F1 in a stopped-flow apparatus. (B) Dose–response relation of the data from (A) ( $\text{IC}_{50} = 0.7 \mu\text{M}$ ). (C) Depolarization-induced  $\text{Ca}^{2+}$  signals evoked by mixing of sperm with KCl-ASW and RU1968F1. Final  $\text{K}^+$  concentration after mixing was 108 mM. (D) Dose–response relation of the data from (C) ( $\text{IC}_{50} = 1.0 \mu\text{M}$ ). (E) Alkaline-evoked  $\text{Ca}^{2+}$  signals in the presence of RU1968F1; the final  $\text{NH}_4\text{Cl}$  concentration after mixing was 30 mM. (F) Dose–response relation of the data from (E) ( $\text{IC}_{50} = 4.6 \mu\text{M}$ ).

the partial inhibition of Slo3 might contribute to this action of RU1968F1.

Finally, we studied the action of RU1968F1 on progesterone-induced changes in swimming behaviour. Incubation of capacitated sperm with progesterone seemingly promoted hyperactivation, which was inhibited by RU1968F1 (Figure 8F); the effect of progesterone was, however, not statistically significant. Therefore, we studied the motility of human sperm before and after rapid activation of CatSper, using caged progesterone (Kilic *et al.*, 2009). Uncaging of progesterone by a brief (200 ms) UV flash instantaneously evoked a wiggly swimming trajectory (Figure 8G) and a decrease of VAP (Figure 8G, I), resembling hyperactivated motility. The VAP reached its minimum ~5 s after uncaging of progesterone and did not recover within the recording time of 10 s. In the presence of RU1968F1, the swimming trajectory and the swimming pattern and VAP

remained unchanged upon uncaging of progesterone (Figure 8H, I). We conclude that progesterone-evoked hyperactivation requires  $\text{Ca}^{2+}$  influx via CatSper.

Furthermore, it is well established that progesterone facilitates the migration of human sperm into viscous medium (Alasmari *et al.*, 2013b). In human sperm lacking functional CatSper channels, this facilitation was abolished (Williams *et al.*, 2015). Using a modified Kremer's sperm-mucus penetration test, we investigated whether inhibition of CatSper by RU1968F1 reproduced this phenotype. To this end, an open glass capillary, which contained medium fortified with methylcellulose, was immersed in a sperm suspension and the number of sperm at a penetration distance of 2 cm (Figure 9A–C) was determined. Data for shorter or longer penetration distances are presented in Supporting Information Figure S8. Consistent with previous results (Alasmari *et al.*, 2013b), bathing sperm in progesterone enhanced the number of sperm

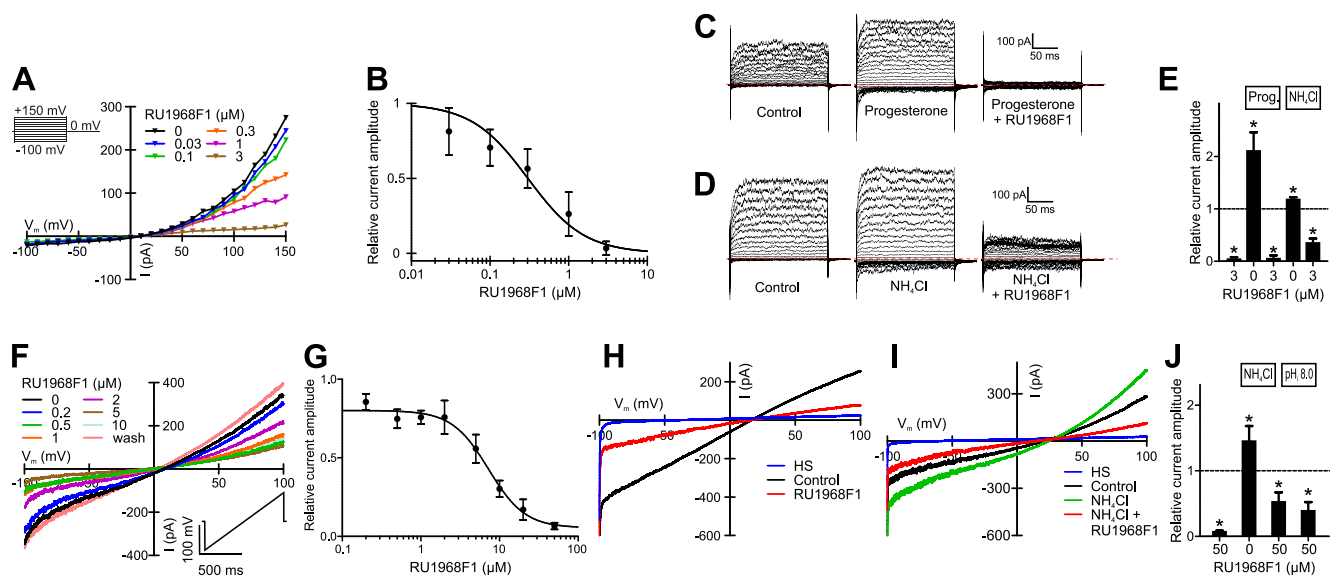


**Figure 6**

RU1968F1 inhibits monovalent cation currents carried by CatSper channels in human and mouse sperm. (A) Representative current–voltage relationship of CatSper currents recorded from a human sperm cell in divalent-free extracellular and intracellular solution (pH 7.4) in the absence and presence of increasing RU1968F1 concentrations. Voltage was stepped from  $-100$  to  $+150$  mV in increments of  $10$  mV. Inset: Voltage protocol. (B) Dose–response relation for the inhibition of human CatSper currents by RU1968F1 at  $+100$  mV ( $IC_{50} = 0.4 \pm 0.3$   $\mu$ M;  $n = 5$ ). (C) Representative monovalent CatSper currents recorded from a human sperm cell before (control) and after perfusion with progesterone ( $2$   $\mu$ M) and progesterone plus RU1968F1 ( $3$   $\mu$ M), evoked by the voltage protocol shown in (A). The dotted red line indicates the current at  $0$  mV. (D) Monovalent CatSper currents recorded from a human sperm cell before (control) and after perfusion with  $NH_4Cl$  ( $10$  mM) and  $NH_4Cl$  plus RU1968F1 ( $3$   $\mu$ M), evoked by the voltage protocol shown in (A). The dotted red line indicates the current at  $0$  mV. (E) Mean amplitudes of monovalent currents at  $+100$  mV recorded in the presence of RU1968F1, progesterone ( $2$   $\mu$ M), progesterone plus RU1968F1,  $NH_4Cl$  ( $10$  mM), and  $NH_4Cl$  plus RU1968F1. Amplitudes were normalized to that evoked in the absence of any drug (control, dashed line). Data shown are means  $\pm$  SD ( $n = 5$ ).  $*P < 0.05$ , significantly different from control. Data were normalized only after performing the statistical analysis using one-way ANOVA (see Methods for details and explanations). (F) Representative CatSper currents recorded from a mouse sperm cell in divalent-free extracellular and intracellular solution (pH 7.2) in the absence and presence of increasing RU1968F1 concentrations. Voltage was ramped between  $-100$  and  $+100$  mV from a holding potential of  $0$  mV. Inset: Voltage protocol. (G) Dose–response relation for the inhibition of mouse CatSper currents at  $+100$  mV ( $IC_{50} = 10 \pm 1$   $\mu$ M,  $n = 3$ ). Data shown are means  $\pm$  SD. (H) Currents in the presence of extracellular divalent ions (HS) and monovalent currents in divalent-free conditions (control) recorded from a mouse sperm cell evoked at pH  $8$  before (control) and after perfusion with RU1968F1, using the voltage protocol shown in (F). (I) Currents recorded from a mouse sperm cell at pH  $7.2$  before (control) and after perfusion with  $NH_4Cl$  ( $30$  mM) and  $NH_4Cl$  plus RU1968F1, using the voltage protocol shown in (F). (J) Mean amplitudes of monovalent currents at  $+100$  mV recorded from mouse sperm in the presence of RU1968F1,  $NH_4Cl$  plus RU1968F1, and at pH  $8$  in the presence of RU1968F1, using the voltage protocol shown in (F). Amplitudes were normalized to the monovalent currents evoked in the absence of any drug (control, dashed line). Data shown are means  $\pm$  SD ( $n = 5$ ).  $*P < 0.05$ , significantly different from control. Data were normalized only after performing the statistical analysis using one-way ANOVA (see Methods for details and explanations).

penetrating the viscous medium (Figure 9A, C, and Supporting Information Figure S8A, C). The effects of progesterone were abolished by  $1$   $\mu$ M RU1968F1 (Figure 9A and Supporting Information Figure S8A). Of note, at this concentration, the drug itself did not affect the number of penetrating cells (Figure 9B and Supporting Information Figure S8B). These effects of progesterone were also abolished when RU1968F1 was added to the capillary medium instead of to the sperm suspension (Figure 9C and Supporting Information Figure S8C). These results support the notion that progesterone acts via CatSper to promote swimming in high-viscosity media and shows that RU1968F1 mimics the lack of functional CatSper channels. Of note, at concentrations  $>1$   $\mu$ M, RU1968F1 in a dose-dependent fashion lowered the number of penetrating sperm both in the absence and presence of progesterone (Figure 9A, B, and Supporting Information Figure S8A, B). This probably reflects

the compound-related decrease of the fraction of progressively motile sperm.

Incubation of human sperm in high micromolar concentrations of progesterone evokes acrosomal exocytosis (Baldi *et al.*, 2009) (Figure 9D), that is, the release of proteolytic enzymes from a secretory vesicle in the sperm head. In the presence of RU1968F1, this action of progesterone was attenuated (Figure 9D), whereas RU1968F1 itself did not evoke acrosomal exocytosis (Figure 9D and Supporting Information Figure S3). These results suggest that the progesterone-induced acrosome reaction involves  $Ca^{2+}$  influx via CatSper and that RU1968F1 might allow the elucidation of the role of CatSper in this process in more detail. Altogether, we conclude that RU1968F1 can provide important insight on the role of progesterone action on CatSper to control sperm function.

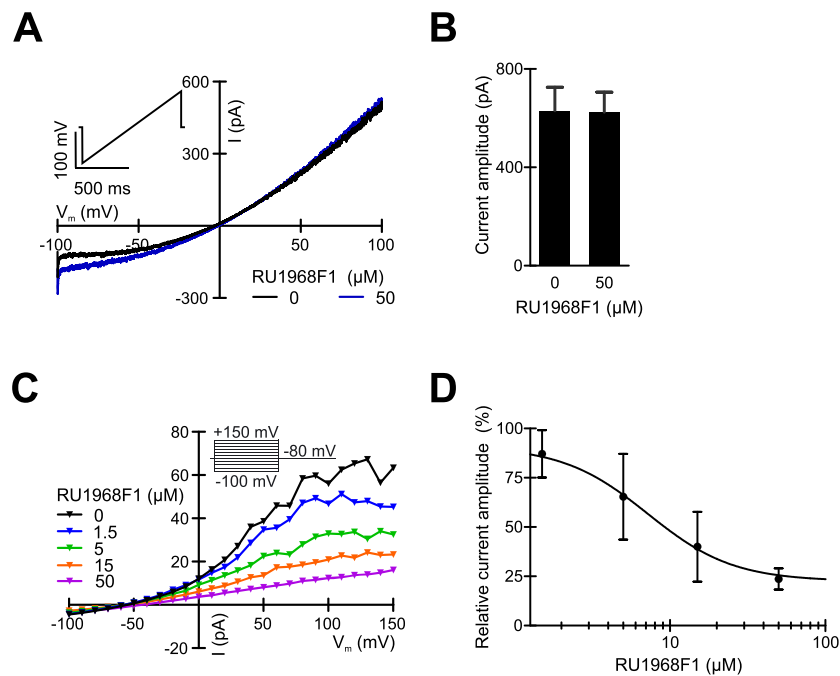


**Figure 7**

RU1968F1 inhibits human but not mouse Slo3 channels. (A) Representative Slo3 currents in a mouse sperm cell, recorded in the presence of extracellular divalent ions at symmetric intra- and extracellular K<sup>+</sup> concentrations in the absence and presence of 50 μM RU1968F1. Inset: Voltage protocol. (B) Mean Slo3 currents in mouse sperm at +100 mV in the absence and presence of 50 μM RU1968F1 ( $n = 5$ ). (C) Representative Slo3 currents recorded from a human sperm cell in the absence and presence of RU1968F1. Inset: Voltage protocol. (D) Dose–response relation for the inhibition of human Slo3 currents by RU1968F1 at +100 mV ( $IC_{50} = 7 \pm 6 \mu\text{M}$ ,  $n = 4$ ). Data shown are means  $\pm$  SD.

### RU1968F1 inhibits chemotaxis of sea urchin sperm

Finally, we tested whether RU1968F1 affected the CatSper-mediated chemotactic steering of sea urchin sperm. In a shallow observation chamber under a dark-field microscope, sperm were bathed in a caged derivative of the chemoattractant resact (Kaupp *et al.*, 2003; Böhmer *et al.*, 2005; Alvarez *et al.*, 2012). A chemoattractant gradient was established by photolysis of caged resact via a UV flash in the centre of the recording chamber (Figure 10A). After the flash, sperm accumulated in the irradiated area, indicated by a decrease of sperm dispersion in the field of view (Figure 10B). Such accumulation was abolished by RU1968F1 (Figure 10), without affecting the overall motility of the sperm.

## Discussion

Here, we introduce RU1968F1 as a new pharmacological tool to elucidate the presence and role of CatSper channels in sperm. RU1968F1 is superior to previously known inhibitors: the compound is relatively selective for CatSper and lacks toxic side effects in human sperm. However, because the action of the compound is complex, we cannot exclude adverse actions in other sperm species. This cautious note has to be considered in further studies of RU1968F1.

What is the molecular mechanism underlying inhibition of CatSper by RU1968F1? It has been proposed that

progesterone acts via an endocannabinoid-signalling pathway, involving the receptor  $\alpha/\beta$  hydrolase domain-containing protein 2 (ABHD2) (Miller *et al.*, 2016). At rest, CatSper is inhibited by the endocannabinoid **2-arachidonoylglycerol (2-AG)** in the flagellar membrane. Upon progesterone binding, ABHD2 degrades 2-AG and, thereby, relieves CatSper from inhibition (Miller *et al.*, 2016). Considering that RU1968F1 is a steroid, this compound might act as an antagonist at the steroid-binding site on ABHD2. However, CatSper channel activation by PGs does not involve ABHD2 (Miller *et al.*, 2016), and in mouse and sea urchin sperm, CatSper channels are not activated by progesterone or PGs (Lishko *et al.*, 2011; Seifert *et al.*, 2015). Moreover, activation of CatSper channels by alkaline pH<sub>i</sub> and depolarization does probably not involve a ligand-binding site. Therefore, we suspect that RU1968F1 binds to residues in the pore region and, thereby, directly block ion flux. The inhibitory action of this compound on classical voltage-gated Ca<sup>2+</sup> channels also supports this conclusion. Of note, the potency of RU1968F1 to inhibit activation of CatSper channels by alkalization seems to decrease with increasing amplitude of  $\Delta\text{pH}_i$ . This might reflect a pH sensitivity of the blocking mechanism or pH-dependent distribution of RU1968F1 across membranes. The latter is rather unlikely. Upon rapid mixing, the compound blocks Ca<sup>2+</sup> influx through CatSper without a measurable latency, suggesting that the compound is more likely to act from the outside. However, the mechanism of CatSper channel inhibition will be difficult to

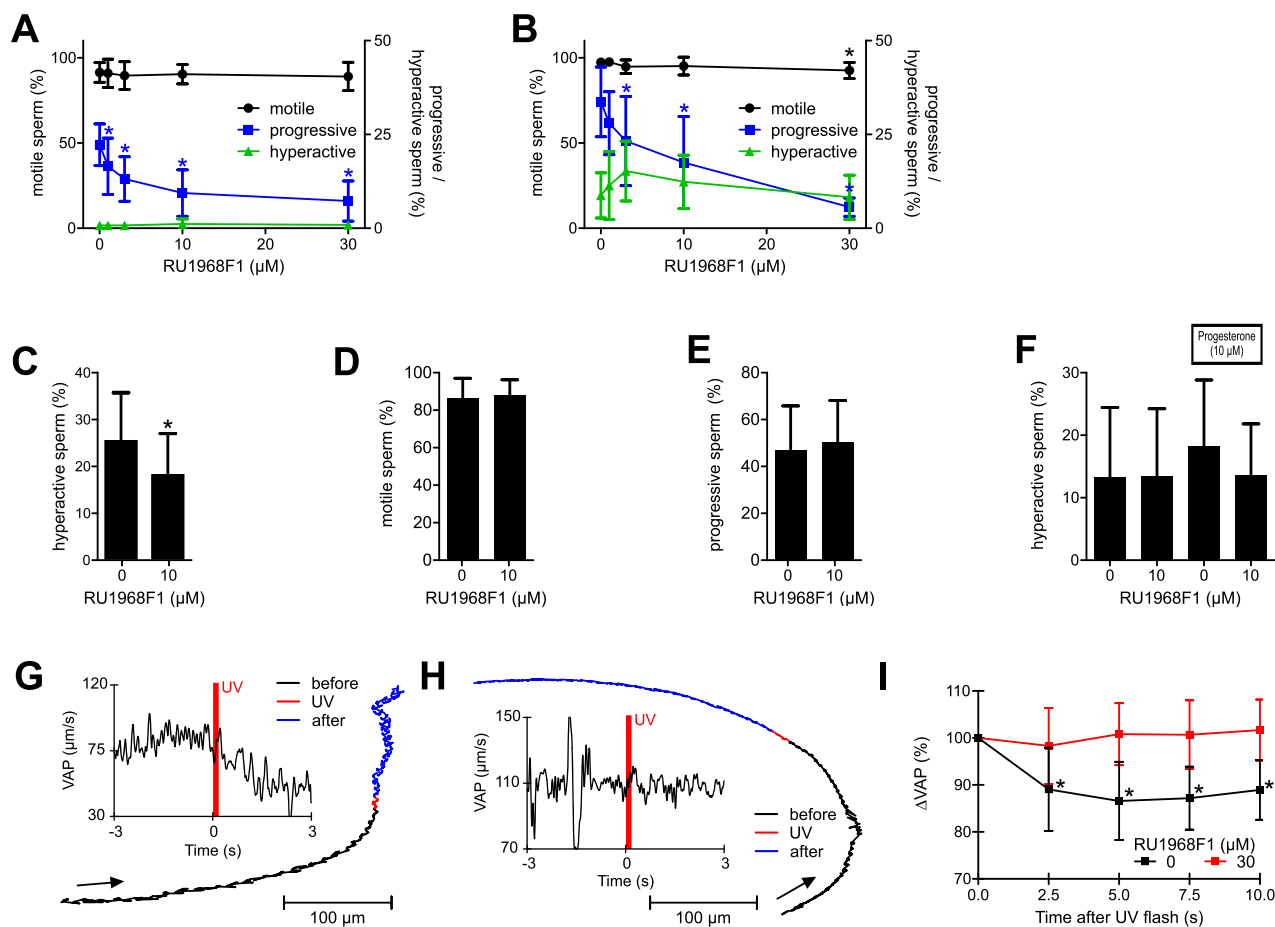


**Figure 8**

RU1968F1 interferes with hyperactivation and abolishes progesterone-induced motility responses in human sperm. (A, B) Motility parameters of non-capacitated (A) and capacitated (B) human sperm in the absence and presence of RU1968F1 ( $n = 8$ ); sperm were bathed in the drug for 300 s. Data shown are means  $\pm$  SD. \* $P < 0.05$ , significantly different from control (absence of RU1968F1). (C–E) Fraction of hyperactivated (C), motile (D), and progressively swimming (E) sperm after capacitation in the absence and presence of RU1968F1 ( $n = 11$ ). Data shown are means  $\pm$  SD. \* $P < 0.05$ , significantly different from control (absence of RU1968F1). (F) Hyperactivation evoked by bathing sperm for 300 s in RU1968F1, progesterone, or progesterone plus RU1968F1 ( $n = 11$ ). Data shown are means  $\pm$  SD. (G) Track of a single sperm cell recorded before (3 s), during (0.2 s) and after (2.8 s) uncaging of progesterone. The arrow indicates the direction of movement. Inset: time course of the VAP; the red bar indicates the uncaging of progesterone. (H) Track of a single sperm cell recorded before (3 s), during (0.2 s, flash), and after (2.8 s) uncaging of progesterone in the presence of RU1968F1 (30  $\mu$ M). Inset: time course of VAP; the red bar indicates the uncaging of progesterone. (I) Mean relative changes in VAP averaged over 20–30 sperm in the field of view after uncaging of progesterone ( $n = 11$ ). Data shown are means  $\pm$  SD. \* $P < 0.05$ , significantly different from control (before flash, 0 s). Data were normalized only after performing the statistical analysis using one-way ANOVA (see Methods for details and explanations).

elucidate rigorously by structure–function analysis or site-directed mutagenesis, because CatSper channels resist functional expression.

What is the nature of the blocking site in Slo3 in human sperm? Human, but not mouse Slo3 channels, are inhibited by micromolar concentrations of progesterone (Brenker *et al.*, 2014). This inhibition results from binding of progesterone either to a site on the channel itself or on its accessory subunit LRRC52 (Brenker *et al.*, 2014). RU1968F1 might act via this steroid-binding site on human Slo3. To improve the selectivity of RU1968F1, a structure–activity analysis is required to identify derivatives that do not act on human Slo3, but display a similar or even enhanced potency to inhibit CatSper. The fact that human Slo3 can be functionally

expressed in cultured cells (Brenker *et al.*, 2014) facilitates this endeavour.

Although the make-up of  $Ca^{2+}$ -signalling pathways in sperm is quite diverse (Kaupp and Strünker, 2016; Alvarez, 2017), the CatSper channel is a common component in many, but not all species (Cai *et al.*, 2014). Our finding that RU1968F1 inhibits CatSper across species opens the possibility to use the compound in a variety of experimental settings. First, teleost fish seem to lack CatSper genes (Cai and Clapham, 2008), although the swimming behaviour of zebrafish is controlled by  $Ca^{2+}$  (Fechner *et al.*, 2015). However, the absence of CatSper channels in fish has been contested (Yanagimachi *et al.*, 2017). RU1968F1 might help to solve this controversy. Second, the genome

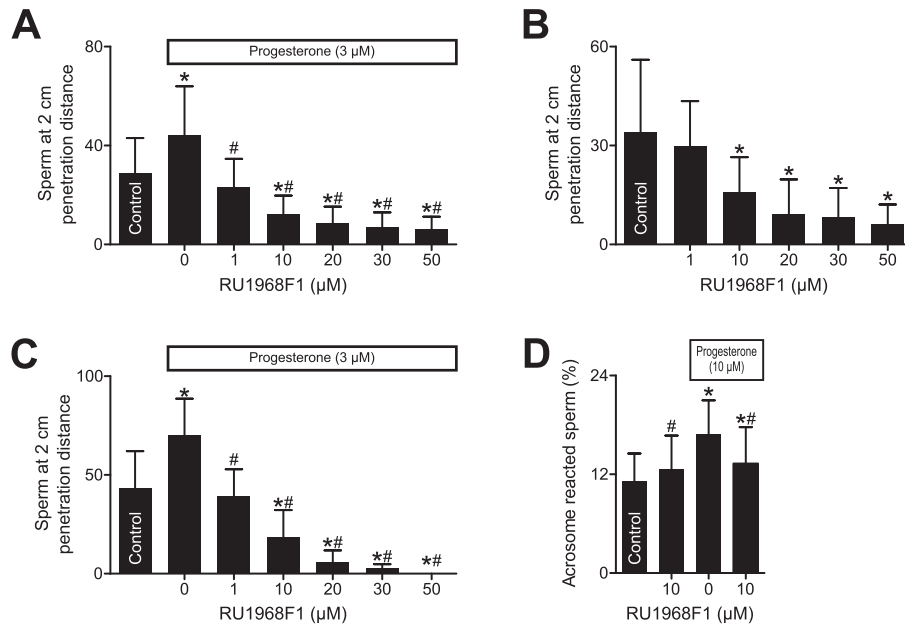


### Figure 9

RU1968F1 suppresses penetration of sperm into viscous media. (A) Number of sperm at a penetration distance of 2 cm in a modified Kremer's sperm–mucus penetration test. The sperm were incubated in buffer (control), progesterone, or progesterone plus RU1968F1 ( $n = 21$ ). Data shown are means  $\pm$  SD. \* $P < 0.05$ , significantly different from control; # $P < 0.05$ , significantly different from progesterone without RU1968F1. (B) Number of sperm after incubation in buffer (control) or RU1968F1 ( $n = 21$ ). Data shown are means  $\pm$  SD. \* $P < 0.05$ , significantly different from control. (C) Number of sperm when the sperm were bathed in buffer (control) or progesterone, in the absence (0) or presence of RU1968F1 in the capillary ( $n = 6$ ). Data shown are means  $\pm$  SD. \* $P < 0.05$ , significantly different from control; # $P < 0.05$ , significantly different from progesterone without RU1968F1. (D) Acrosome reaction evoked by RU1968F1, progesterone, or progesterone and RU1968F1 ( $n = 10$ ). Data shown are means  $\pm$  SD. \* $P < 0.05$ , significantly different from control, # $P < 0.05$ , significantly different from progesterone.

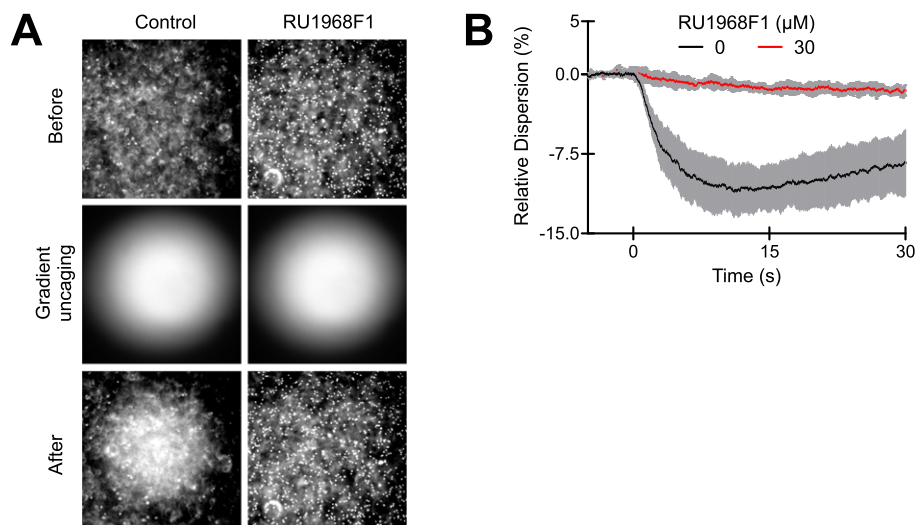


### Figure 10

RU1968F1 abolishes chemotaxis of sea urchin sperm. (A) Dark-field microscopy images of a sperm suspension before (top) and after (bottom) establishing a resact gradient by photolysis of caged resact (middle) in the absence (control, left panel) or presence of RU1968F1 (30  $\mu$ M, right panel). RU1968F1 abolishes resact-induced sperm accumulation. (B) Relative change of the sperm dispersion in the field of view evoked by uncaging of resact ( $t = 0$ , flash) in the absence (control) or presence of RU1968F1; a decrease of dispersion indicates sperm accumulation in the irradiated area (control,  $n = 5$ , RU1968F1,  $n = 6$ ). Data shown are means  $\pm$  SD.

of many marine species, including the saprophytic fungus *Allomyces macrogynus*, the tunicate *Ciona intestinalis* and the seastar *Asterias amurensis* harbour CatSper genes (Cai and Clapham, 2008; Cai *et al.*, 2014). Sperm from these species also undergo chemotaxis (Miller, 1975; Pommerville, 1978; Yoshida *et al.*, 2002; Matsumoto *et al.*, 2003). RU1968F1 might reveal whether chemotaxis involves CatSper. Third, the drug might help to define the diverse functions of CatSper among mammalian sperm. For example, mouse sperm undergo rotational motion that governs rheotaxis in gradients of flow velocities (Miki and Clapham, 2013). By contrast, CatSper<sup>-/-</sup> mouse sperm do not rotate and fail to undergo rheotaxis, suggesting that Ca<sup>2+</sup> influx via CatSper channels is required. However, another study describes rheotaxis as a passive process that does not require Ca<sup>2+</sup> influx (Zhang *et al.*, 2016). CatSper recruit several proteins into Ca<sup>2+</sup>-signalling domains that form a quadrilateral arrangement along the flagellar membrane (Chung *et al.*, 2014; Chung *et al.*, 2017). Targeted deletion of CatSper subunits disrupts these signalling domains (Chung *et al.*, 2014; Chung *et al.*, 2017). Therefore, the motility defects of CatSper<sup>-/-</sup> mouse sperm might be caused by the lack of Ca<sup>2+</sup> influx via CatSper, by disruption of the supramolecular flagellar ultrastructure, or by a combination of both. Fourth, in human sperm, neither the role of oviductal CatSper ligands nor the role of CatSper during fertilization has been fully established. This is due to the demanding challenge to mimic the complex chemical, hydrodynamic and topographical environment of the oviduct *in vitro* (Xiao *et al.*, 2017). We envision the use of RU1968F1 as a tool to study the role of CatSper and its ligands in human sperm, navigating across artificial or explanted oviducts.

Finally, mutations in *CATSPER* genes (Avenarius *et al.*, 2009; Hildebrand *et al.*, 2010) and the lack of functional CatSper channels (Williams *et al.*, 2015) are associated with male infertility. In human sperm, at least *in vitro*, RU1968F1 mimics the lack of CatSper channels, indicating that inhibition of these channels *in vivo* might prevent fertilization. Thus, RU1968F1 could serve as a lead structure to develop new non-hormonal contraceptives. Drugs that specifically target CatSper should exhibit no side effects, because the expression of the channel is confined to sperm.

## Acknowledgements

This work was supported by the German Research Foundation (SFB645 to T.S., U.B.K. and D.W.; SFB1089 to U.B.K.; SPP1926, 1726 and TRR83 to D.W.; and CRU326 to T.S.); the Cells-in-Motion (CiM) Cluster of Excellence, Münster (FF-2016-17 to T.S.); the ImmunoSensation Cluster of Excellence, Bonn (to U.B.K. and D.W.); the Fritz-Thyssen-Foundation and the Boehringer Ingelheim Foundation (to D.W.), the fund Innovative Medical Research (IMF) of the University of Münster Medical School, Münster, (I-BR121507 to C.B.); and the CAPES Foundation (Ministry of Education, Brazil, to E.T.N.). We thank David Clapham (Janelia Research Campus, USA) for kindly providing the CatSper1-KO mice.

## Author contributions

A.R. and T.S. conceived and designed the study, coordinated the experiments and wrote the manuscript. A.R., C.S., C.B., D.F., T.E.N., Y.M.C., L.T., M.B., G.S., T.K.B., M.K., L.A., D.W., X.H.Z., E.B., S.P., U.B.K. and T.S. acquired, analysed and/or interpreted data and revised the manuscript critically for important intellectual content. All authors approved the manuscript.

## Conflict of interest

The authors declare no conflicts of interest.

## Declaration of transparency and scientific rigour

This Declaration acknowledges that this paper adheres to the principles for transparent reporting and scientific rigour of preclinical research recommended by funding agencies, publishers and other organisations engaged with supporting research.

## References

- Alasmari W, Barratt CLR, Publicover SJ, Whalley KM, Foster E, Kay V *et al.* (2013a). The clinical significance of calcium-signalling pathways mediating human sperm hyperactivation. *Hum Reprod* 28: 866–876.
- Alasmari W, Costello S, Correia J, Oxenham SK, Morris J, Fernandes L *et al.* (2013b). Ca<sup>2+</sup> signals generated by CatSper and Ca<sup>2+</sup> stores regulate different behaviors in human sperm. *J Biol Chem* 288: 6248–6258.
- Alexander SPH, Striessnig J, Kelly E, Marrion NV, Peters JA, Faccenda E *et al.* (2017a). The Concise Guide to PHARMACOLOGY 2017/18: Voltage-gated ion channels. *Br J Pharmacol* 174 (Suppl 1): S160–S194.
- Alexander SPH, Peters JA, Kelly E, Marrion NV, Faccenda E, Harding SD *et al.* (2017b). The Concise Guide to PHARMACOLOGY 2017/18: Ligand-gated ion channels. *Br J Pharmacol* 174: S130–S159.
- Alvarez L (2017). The tailored sperm cell. *J Plant Res* 130: 455–464.
- Alvarez L, Dai L, Friedrich BM, Kashikar ND, Gregor I, Pascal R *et al.* (2012). The rate of change in Ca<sup>2+</sup> concentration controls sperm chemotaxis. *J Cell Biol* 196: 653–663.
- Alvarez L, Friedrich BM, Gompper G, Kaupp UB (2014). The computational sperm cell. *Trends Cell Biol* 24: 198–207.
- Ananchenko SN, Limanov VY, Leonov VN, Rzhiznikov VN, Torgov IV (1962). Syntheses of derivatives of oestrone and 19-norsteroids from 6-methoxytetralone and 6-hydroxytetralone. *Tetrahedron* 18: 1355–1367.
- Ananchenko SN, Torgov IV (1963). New syntheses of estrone, d,1-8-iso-oestrone and d,1-19-noresterone. *Tetrahedron Lett* 4: 1553–1558.
- Avenarius MR, Hildebrand MS, Zhang Y, Meyer NC, Smith LLH, Kahrizi K *et al.* (2009). Human male infertility caused by mutations in the *CATSPER1* channel protein. *Am J Hum Genet* 84: 505–510.

- Baldi E, Luconi M, Muratori M, Marchiani S, Tamburrino L, Forti G (2009). Nongenomic activation of spermatozoa by steroid hormones: facts and fiction. *Mol Cell Endocrinol* 308: 39–46.
- Böhmer M, Van Q, Weyand I, Hagen V, Beyermann M, Matsomoto M *et al.* (2005).  $\text{Ca}^{2+}$  spikes in the flagellum control chemotactic behavior of sperm. *EMBO J* 24: 2741–2752.
- Brenker C, Goodwin N, Weyand I, Kashikar ND, Naruse M, Krähling M *et al.* (2012). The CatSper channel: a polymodal chemosensor in human sperm. *EMBO J* 31: 1654–1665.
- Brenker C, Zhou Y, Müller A, Echeverry FA, Trötschel C, Poetsch A *et al.* (2014). The  $\text{Ca}^{2+}$ -activated  $\text{K}^+$  current of human sperm is mediated by Slo3. *Elife* 3: e01438.
- Brenker C, Schiffer C, Wagner IV, Tüttelmann F, Röpke A, Rennhack A *et al.* (2018). Action of steroids and plant triterpenoids on CatSper  $\text{Ca}^{2+}$  channels in human sperm. *Proc Natl Acad Sci U S A* 115: E344–E346.
- Cai X, Clapham DE (2008). Evolutionary genomics reveals lineage-specific gene loss and rapid evolution of a sperm-specific ion channel complex: CatSper and CasSper $\beta$ . *PLoS One* 3: e3569.
- Cai X, Wang X, Clapham DE (2014). Early evolution of the eukaryotic  $\text{Ca}^{2+}$  signaling machinery: conversation of the CatSper channel complex. *Mol Biol Evol* 31: 2735–2740.
- Carlson AE, Burnett LA, del Camino D, Quill TA, Hille B, Chong JA *et al.* (2009). Pharmacological targeting of native CatSper channels reveals a required role in maintenance of sperm hyperactivation. *PLoS One* 4: e6844.
- Carlson AE, Quill TA, Westenbroek RE, Schuh SM, Hille B, Babcock DF (2005). Identical phenotypes of CatSper1 and CatSper2 null sperm. *J Biol Chem* 280: 32238–32244.
- Carlson AE, Westenbroek RE, Quill TA, Ren D, Clapham DE, Hille B *et al.* (2003). CatSper1 required for evoked  $\text{Ca}^{2+}$  entry and control of flagellar function in sperm. *Proc Natl Acad Sci U S A* 100: 14864–14868.
- Chávez JC, De la Vega-Beltrán JL, José O, Torres P, Nishigaki T, Treviño CL *et al.* (2017). Acrosomal alkalization triggers  $\text{Ca}^{2+}$  release and acrosome reaction in mammalian spermatozoa. *J Cell Physiol*. <https://doi.org/10.1002/jcp.26262>.
- Chung JJ, Miki M, Kim D, Shim SH, Shi HF, Hwang JY *et al.* (2017). CatSper $\zeta$  regulates the structural continuity of sperm  $\text{Ca}^{2+}$  signaling domains and is required for normal fertility. *Elife* 6: e23082.
- Chung JJ, Navarro B, Krapivinsky G, Krapivinsky L, Clapham DE (2011). A novel gene required for male fertility and functional CatSper channel formation in spermatozoa. *Nat Commun* 2: 153.
- Chung JJ, Shim SH, Everley RA, Gygi SP, Zhuang X, Clapham DE (2014). Structurally distinct  $\text{Ca}^{2+}$  signaling domains of sperm flagella orchestrate tyrosine phosphorylation and motility. *Cell* 157: 808–822.
- Curtis MJ, Alexander S, Cirino G, Docherty JR, George CH, Giembycz MA *et al.* (2018). Experimental design and analysis and their reporting II: updated and simplified guidance for authors and peer reviewers. *Brit J Pharmacol* 175: 987–993.
- Espinal-Enríquez J, Priego-Espinosa DA, Darszon A, Beltrán C, Martínez-Mekler G (2017). Network model predicts that CatSper is the main  $\text{Ca}^{2+}$  channel in the regulation of sea urchin sperm motility. *Sci Rep* 7: 4236.
- Fechner S, Alvarez L, Bönigk W, Müller A, Berger TK, Pascal R *et al.* (2015). A  $\text{K}^+$ -selective CNG channel orchestrates  $\text{Ca}^{2+}$  signaling in zebrafish sperm. *Elife* 4: e07624.
- Harding SD, Sharman JL, Faccenda E, Southan C, Pawson AJ, Ireland S *et al.* (2018). The IUPHAR/BPS Guide to PHARMACOLOGY in 2018: updates and expansion to encompass the new guide to IMMUNOPHARMACOLOGY. *Nucl Acids Res* 46: D1091–D1106.
- Harper CV, Kirkman-Brown JC, Barratt CLR, Publicover SJ (2003). Encoding of progesterone stimulus intensity by intracellular  $[\text{Ca}^{2+}]_i$  in human spermatozoa. *Biochem J* 372: 407–417.
- Hildebrand MS, Avenarius MR, Fellous M, Zhang Y, Meyer NC, Auer J *et al.* (2010). Genetic male infertility and mutation of CatSper ion channels. *Eur J Hum Genet* 18: 1178–1184.
- Ho K, Wolff CA, Suarez SS (2009). CatSper-null mutant spermatozoa are unable to ascend beyond the oviductal reservoir. *Reprod Feril Dev* 21: 345–350.
- Kaupp UB, Solzin J, Hildebrand E, Brown JE, Helbig A, Hagen V *et al.* (2003). The signal flow and motor response controlling chemotaxis of sea urchin sperm. *Nat Cell Biol* 5: 109–117.
- Kaupp UB, Strünker T (2016). Signaling in sperm: more different than similar. *Trends Cell Biol* 27: 101–109.
- Kilic F, Kashikar ND, Schmidt R, Alvarez L, Dai L, Weyand I *et al.* (2009). Caged progesterone: a new tool for studying rapid nongenomic actions of progesterone. *J Am Chem Soc* 131: 4027–4030.
- Kilkenny C, Browne W, Cuthill IC, Emerson M, Altman DG (2010). Animal research: reporting in vivo experiments: the ARRIVE guidelines. *Br J Pharmacol* 160: 1577–1579.
- Kirichok Y, Navarro B, Clapham DE (2006). Whole-cell patch-clamp measurements of spermatozoa reveal an alkaline-activated  $\text{Ca}^{2+}$  channel. *Nature* 439: 737–740.
- Lishko PV, Botchkina IL, Federenko A, Kirichok Y (2010). Acid extrusion from human spermatozoa is mediated by flagellar voltage-gated proton channel. *Cell* 140: 327–337.
- Lishko PV, Botchkina IL, Kirichok Y (2011). Progesterone activates the principal  $\text{Ca}^{2+}$  channel of human sperm. *Nature* 471: 387–391.
- Liu J, Xia J, Cho KH, Clapham DE, Ren D (2007). CatSper $\beta$ , a novel transmembrane protein in the CatSper channel complex. *J Biol Chem* 282: 18945–18952.
- Loux SC, Crawford KR, Ing NH, Gonzales-Fernandez L, Macias-Garcia B, Love C *et al.* (2013). CatSper and the relationship of hyperactivated motility to intracellular calcium and pH kinetics in equine sperm. *Biol Reprod* 89: 123.
- Mansell SA, Publicover SJ, Barratt CLR, Wilson SM (2014). Patch clamp studies of human sperm under physiological ionic conditions reveal three functionally and pharmacologically distinct cation channels. *Mol Hum Reprod* 20: 392–408.
- Matsumoto M, Solzin J, Helbig A, Hagen V, Ueno SI, Kawase O *et al.* (2003). A sperm-activating peptide controls a cGMP-signaling pathway in starfish sperm. *Dev Biol* 260: 314–324.
- McGrath JC, Lilley E (2015). Implementing guidelines on reporting research using animals (ARRIVE etc.): new requirements for publication in BJP. *Br J Pharmacol* 172: 3189–3193.
- Miki M, Clapham DE (2013). Rheotaxis guides mammalian sperm. *Curr Biol* 23: 443–452.
- Miller MR, Mannowetz N, Iavarone AT, Safavi R, Gracheva EO, Smith JF *et al.* (2016). Unconventional endocannabinoid signaling governs sperm activation via the sex hormone progesterone. *Science* 352: 555–559.
- Miller RL (1975). Chemotaxis of the spermatozoa of *Ciona intestinalis*. *Nature* 254: 244–245.



- Mortimer ST, Swan MA, Mortimer D (1998). Effect of seminal plasma on capacitation and hyperactivation in human spermatozoa. *Hum Reprod* 13: 2139–2146.
- Navarro B, Kirichok Y, Clapham DE (2007). K<sub>Sper</sub>, a pH-sensitive K<sup>+</sup> current that controls sperm membrane potential. *Proc Natl Acad Sci U S A* 104: 7688–7692.
- Navarro B, Miki K, Clapham DE (2011). ATP-activated P2X<sub>2</sub> current in mouse spermatozoa. *Proc Natl Acad Sci U S A* 108: 14342–14347.
- Oren-Benaroya R, Orvieto R, Gakamsky A, Pinchasov M, Eisenbach M (2008). The sperm chemoattractant secreted from human cumulus cells is progesterone. *Hum Reprod* 23: 2339–2345.
- Pommerville J (1978). Analysis of gamete and zygote motility in *allomyces*. *Exp Cell Res* 113: 161–172.
- Publicover SJ, Giojalas LC, Teves ME, Mendes Machado de Oliveira GS, Morales Garcia AA, Barratt CLR *et al.* (2008). Ca<sup>2+</sup> signaling in the control of motility and guidance in mammalian sperm. *Front Biosci* 13: 5623–5637.
- Qi H, Moran MM, Navarro B, Chong JA, Krapivinsky G, Krapivinsky L *et al.* (2007). All four CatSper ion channel proteins are required for male fertility and sperm cell hyperactivated motility. *Proc Natl Acad Sci U S A* 104: 1219–1223.
- Quill TA, Ren D, Clapham DE, Garbers DL (2001). A sperm ion channel required for sperm motility and male fertility. *Nature* 413: 603–609.
- Ren D, Navarro B, Perez G, Jackson AC, Hsu S, Shi Q *et al.* (2001). A sperm ion channel required for sperm motility and male fertility. *Nature* 413: 603–609.
- Santi CM, Martinez-Lopez P, De la Vega-beltran JL, Butler A, Alisio A, Darszon A *et al.* (2010). The Slo3 sperm-specific potassium channel plays a vital role in male fertility. *FEBS Lett* 584: 1041–1046.
- Schaefer M, Habenicht UF, Bräutigam M, Gudermann T (2000). Steroidal sigma receptor ligands affect signaling pathways in human spermatozoa. *Biol Reprod* 63: 57–63.
- Schaefer M, Hofmann T, Schultz G, Gudermann T (1998). A new prostaglandin E receptor mediates calcium influx and acrosome reaction in human spermatozoa. *Proc Natl Acad Sci U S A* 95: 3008–3013.
- Schiffer C, Müller A, Egeberg DL, Alvarez L, Brenker C, Rehfeld A *et al.* (2014). Direct action of endocrine disrupting chemicals on human sperm. *EMBO Rep* 15: 758–765.
- Schuetz AW, Dubin NH (1981). Progesterone and prostaglandin secretion by ovulated rat cumulus cell-oocyte complexes. *Endocrinology* 108: 457–463.
- Seifert R, Flick M, Bönigk W, Alvarez L, Trötschel C, Poetsch A *et al.* (2015). The CatSper channel controls chemosensation in sea urchin sperm. *EMBO J* 34: 379–392.
- Strünker T, Goodwin N, Brenker C, Kashikar ND, Weyand I, Seifert R *et al.* (2011). The CatSper channel mediates progesterone induced Ca<sup>2+</sup> influx in human sperm. *Nature* 471: 382–386.
- Suarez SS (2008). Control of hyperactivation in sperm. *Hum Reprod Update* 14: 647–657.
- Tamburrino L, Marchiani S, Minetti F, Forti G, Muratori M, Baldi E (2014). The CatSper calcium channel in human sperm: relation with motility and involvement in progesterone-induced acrosome reaction. *Hum Reprod* 29: 418–428.
- Tamburrino L, Marchiani S, Vicini E, Muciaccia B, Cambi M, Pellegrini S *et al.* (2015). Quantification of CatSper1 expression in human spermatozoa and relation to functional parameters. *Hum Reprod* 30: 1532–1544.
- Van Leusen D, Van Leusen AM (2004). Synthetic uses of tosylmethyl isocyanide (TosMic). *Organic Reactions* 57: 417–666.
- Wang H, Liu J, Cho KH, Ren D (2009). A novel, single, transmembrane protein CatSper<sub>γ</sub> is associated with CatSper1 channel protein. *Biol Reprod* 81: 539–544.
- Williams HL, Mansell S, Alasmari W, Brown SG, Wilson SM, Sutton KA *et al.* (2015). Specific loss of CatSper function is sufficient to compromise fertilization capacity of human spermatozoa. *Hum Reprod* 30: 2737–2746.
- WHO (2010). World Health Organization Department of Reproductive Health and Research. WHO laboratory manual for the examination and processing of human semen, fifth edition.
- Yanagimachi R, Harumi T, Matsubara H, Yan W, Yuan S, Hirohashi N *et al.* (2017). Chemical and physical guidance of fish spermatozoa into the egg through the micropyle. *Biol Reprod* 96: 780–799.
- Xiao S, Copetta JR, Rogers HB, Isenberg BC, Zhu J, Olalekan SA *et al.* (2017). A microfluidic culture model of the human reproductive tract and 28-day menstrual cycle. *Nat Commun* 8: 14584.
- Yoshida M, Murata M, Inaba K, Morisawa M (2002). A chemoattractant for ascidian spermatozoa is a sulfated steroid. *Proc Natl Acad Sci U S A* 99: 14831–14836.
- Zhang Z, Liu J, Meriano J, Ru C, Xie S, Luo J *et al.* (2016). Human sperm rheotaxis: a passive physical process. *Sci Rep* 6: 23553.
- Zeng XH, Navarro B, Xia XM, Clapham DE, Lingle CJ (2013). Simultaneous knockout of Slo3 and CatSper1 abolishes all alkalization- and voltage-activated currents in mouse spermatozoa. *J Gen Physiol* 142: 305–313.
- Zeng XH, Yang C, Kim ST, Lingle CJ, Xia XM (2011). Deletion of the Slo3 gene abolishes alkalization-activated K<sup>+</sup> current in mouse spermatozoa. *Proc Natl Acad Sci U S A* 108: 5879–5884.

## Supporting Information

Additional supporting information may be found online in the Supporting Information section at the end of the article.

<https://doi.org/10.1111/bph.14355>

**Figure S1** Relative stereochemistry at C18 and C20 in 3a. Right panel: H-H COESY spectrum of 3a. C18-CH<sub>3</sub> groups were identified as singlets at  $\delta = 0.73$  ppm (blue, major isomer) and  $\delta = 0.80$  ppm (red, minor isomer). CH<sub>3</sub> groups at C21 were identified as overlapping doublets ( $\delta = 1.09$  ppm major isomer and  $\delta = 1.10$  ppm minor isomer), each of which could be cross-referenced to a multiplet at  $\delta > 2.5$  ppm, which consequently was assigned to the CH-group at C20. (Major isomer, dashed blue lines,  $\delta = 1.09$  ppm  $\rightarrow$   $\delta = 2.64$  ppm; minor isomer, dashed red lines,  $\delta = 1.10$  ppm  $\rightarrow$   $\delta = 2.76$  ppm). Left panel: NOE experiments to assign relative stereochemistry between C18 and C20. Blue box: major isomer; irradiation of the C18-CH<sub>3</sub> singlet ( $\delta = 0.73$  ppm) results in a strong negative NOE resonance at  $\delta = 2.64$  ppm, indicating spatial proximity of C18- and C20-protons. Cis configuration was assigned for this isomer. Red box: minor isomer; irradiation of the C18-CH<sub>3</sub> singlet ( $\delta = 0.80$  ppm) results in no observable NOE resonance at  $\delta = 2.76$  ppm, indicating no spatial

proximity of C18- and C20-protons. Trans configuration was assigned for this isomer.

**Figure S2** Relative stereochemistry at C18 and C20 in 3b. Right panel: H-H COESY spectrum of 3b. C18-CH3 groups are easily identified as singlets at  $\delta = 0.72$  ppm (blue, major isomer) and  $\delta = 0.85$  ppm (red, minor isomer). CH3 groups at C21 are identified as doublets ( $\delta = 1.16$  ppm major isomer and  $\delta = 1.05$  ppm minor isomer), each of which could be cross referenced to a multiplet at  $\delta > 2.5$  ppm, which consequently was assigned to the CH-group at C20. (Major isomer, dashed blue lines,  $\delta = 1.16$  ppm  $\rightarrow$   $\delta = 2.55$  ppm; minor isomer, dashed red lines,  $\delta = 1.05$  ppm  $\rightarrow$   $\delta = 2.64$  ppm). Left panel: NOE experiments to assign relative stereochemistry between C18 and C20. Blue box: major isomer; irradiation of the C18-CH3 singlet ( $\delta = 0.72$  ppm) results in a strong negative NOE resonance at  $\delta = 2.55$  ppm, indicating spatial proximity of C18- and C20-protons. Cis configuration was assigned for this isomer. Red box: minor isomer; irradiation of the C18-CH3 singlet ( $\delta = 0.85$  ppm) results in no observable NOE resonance at  $\delta = 2.64$  ppm, indicating no spatial proximity of C18- and C20-protons. Trans configuration was assigned for this isomer.

**Figure S3** The action of RU1968F1 itself in human sperm. (A) RU1968F1-induced  $\text{Ca}^{2+}$  signals in human sperm. (B) Dose-response relation of the RU1968F1-evoked signal amplitudes ( $n = 3$ ). Error bars indicate SD. (C) RU1968F1-induced  $\text{Ca}^{2+}$  signals in human sperm at 10 nM extracellular  $\text{Ca}^{2+}$ . (D) Changes in  $\text{pH}_i$  evoked by RU1968F1 or  $\text{NH}_4\text{Cl}$  in sperm loaded with the pH indicator BCECF. The signals were recorded in the FluoStar. (E) Fraction of immotile sperm in the absence ( $n = 9$ ) and presence of the RU1968F1 (30  $\mu\text{M}$ ), MDL12330A (100  $\mu\text{M}$ ), Mibefradil (60  $\mu\text{M}$ ), or NNC-55-0396 (30  $\mu\text{M}$ ) ( $n = 5$ ). Error bars indicate SD.  $*P < 0.05$  versus control. (F) Fraction of vital cells in the absence and presence of the inhibitors ( $n = 5$ ). Vitality was evaluated by the Eosin test, performed according to the WHO manual. Error bars indicate SD.  $*P < 0.05$  versus control (G) Fold increase in acrosome-reacted sperm after treatment with RU1968F1 (30  $\mu\text{M}$ ), Mibefradil (40  $\mu\text{M}$ ), or NNC-55-0396 (20  $\mu\text{M}$ ) ( $n = 10$ ). Error bars indicate SD.  $*P < 0.05$  versus control.

**Figure S4** RU1968F1 inhibits depolarization- and alkaline-evoked  $\text{Ca}^{2+}$  signals in human sperm. (A)  $\text{Ca}^{2+}$  signals evoked by mixing of sperm with pH 8.6-HTF and RU1968F1 in a stopped-flow apparatus. The final pH after mixing was 8.1. (B)  $\text{Ca}^{2+}$  signals evoked by mixing of sperm with  $\text{K}^+$ -HTF and RU1968F1 in a stopped-flow apparatus. The final  $\text{K}^+$  concentration after mixing was 51.25 mM.

**Figure S5** RU1968F1 inhibits progesterone responses in sperm bathed in  $\text{NH}_4\text{Cl}$ . (A) Progesterone-induced  $\text{Ca}^{2+}$  signals (500 nM) in human sperm bathed for 20 min in 30 mM  $\text{NH}_4\text{Cl}$ . (B) Dose-response relation of signals from (A). Mean  $\text{IC}_{50}$ :  $3.1 \pm 1.2$  ( $n = 5$ ).

**Figure S6** Action of RU1968F2-F4 on their own and on CatSper-mediated  $\text{Ca}^{2+}$  signals in human sperm populations. (A) RU1968F2-induced  $\text{Ca}^{2+}$  signals in human sperm. (B) Progesterone (500 nM)-induced  $\text{Ca}^{2+}$  signals in human sperm in the presence of RU1968F2; (C) Dose-response relation of the signal amplitudes from (B) ( $\text{IC}_{50} = 1.6$   $\mu\text{M}$ ). (D) RU1968F3-induced

$\text{Ca}^{2+}$  signals in human sperm. (E) Progesterone-induced  $\text{Ca}^{2+}$  signals in the presence of RU1968F3. (F) Dose-response relation of the signal amplitudes from (E) ( $\text{IC}_{50} = 2.7$   $\mu\text{M}$ ). (G) RU1968F4-induced  $\text{Ca}^{2+}$  signals in human sperm. (H) Progesterone-induced  $\text{Ca}^{2+}$  signals in human sperm in the presence of RU1968F4. (I) Dose-response relation of the signal amplitudes from (H) ( $\text{IC}_{50} = 5.8$   $\mu\text{M}$ ).

**Figure S7** Action of RU1968F1 on Hv1 currents in human sperm and ATP-evoked  $\text{Ca}^{2+}$  responses in mouse sperm. (A) Voltage-gated proton currents recorded from a human sperm cell before (blue) and after superfusion with RU1968F1 (red). (B) Mean outward current before and after application of RU1968F1 ( $n = 3$ ). Arrow in panel (A) indicates the time point at which outward currents were determined. Error bars indicate SD. (C) ATP-evoked  $\text{Ca}^{2+}$  signals in CatSper1<sup>-/-</sup> mouse sperm in the absence and presence of RU1968F1. The  $\text{Ca}^{2+}$  responses were recorded in the FluoStar. ATP was injected at  $t = 0$  s.

**Figure S8** RU1968F1 suppresses penetration of sperm into viscous media. (A) Number of sperm at penetration distances of 0–4 cm in a modified Kremer's sperm-mucus penetration test. Sperm were incubated in buffer (0) or RU1968F1 ( $n = 21$ ). Error bars indicate SD.  $*P < 0.05$  versus control (0, without RU1968F1).  $\#P < 0.05$  versus progesterone without RU1968F1 (B) Number of sperm after incubation in buffer (0), progesterone, or progesterone plus RU1968F1 ( $n = 21$ ). Error bars indicate SD.  $*P < 0.05$  versus control,  $\#P < 0.05$  versus progesterone without RU1968F1 (0, without progesterone). (C) Number of sperm bathed in buffer (control) or progesterone when the capillary included buffer (0) or RU1968F1 ( $n = 6$ ). Error bars indicate SD.  $*P < 0.05$  versus control (0, without progesterone),  $\#P < 0.05$  versus progesterone without RU1968F1 (0, without progesterone).

**Figure S9** RU1968F1 inhibits  $\text{Ca}_v1.2$  channels. Representative whole-cell current recorded from a HEK293T cell expressing human  $\text{Ca}_v1.2 + \beta 2b + \alpha 2\delta 1$  before (A) and after perfusion of the cell with 50  $\mu\text{M}$  RU1968F1 (B). (C) Plotting the mean peak current versus voltage demonstrates the incomplete block of  $\text{Ca}_v1.2$  by RU1968F1 ( $n = 5$ ). (D) Peak currents at +20 mV recorded every 2 s while the cell was perfused with external solution or solution containing 50  $\mu\text{M}$  RU1968F1. The reduction and recovery of the current during the wash-in (red) and wash-out (blue) of RU1968F1, respectively, was fitted with an exponential function. The time constants were used to calculate an approximate affinity ( $k_D$ ) of  $31 \pm 9$   $\mu\text{M}$  ( $n = 4$ ).

**Figure S10** RU1968F1 inhibits  $\text{Ca}_v3.2$  channels. Representative whole-cell current recorded from a HEK293T cell expressing  $\text{Ca}_v3.2$  before (A) and after perfusion of the cell with RU1968F1 (B). (C) Plotting the mean peak current versus voltage demonstrates the incomplete block of  $\text{Ca}_v3.2$  by RU1968F1 ( $n = 5$ ). (D) Peak currents at +20 mV recorded every 2 s while the cell was perfused with external solution or solution containing 50  $\mu\text{M}$  RU1968F1. The reduction and recovery of the current during the wash-in (red) and wash-out (blue) of RU1968F1, respectively, was fitted with an exponential function. The time constants were used to calculate an approximate affinity ( $k_D$ ) of  $16 \pm 3$   $\mu\text{M}$  ( $n = 4$ ).